Available online at www.sciencedirect.com
SCIENCE DIRECT®
Journal of Computational Physics 207 (2005) 28–51
JOURNAL OF COMPUTATIONAL PHYSICS
www.elsevier.com/locate/jcp

# Discretization of Dirac delta functions in level set methods

Björn Engquist [a,1], Anna-Karin Tornberg [b,*,2], Richard Tsai [c,3]

[a] Department of Mathematics and PACM, Princeton University, Fine Hall, Princeton, NJ 08544-1000, USA
[b] Courant Institute of Mathematical Sciences, New York University, 251 Mercer Street, New York, 10012-1185, USA
[c] Institute for Advanced Study and Department of Mathematics, Princeton University. Fine Hall, Princeton, 08544-1000, USA

Received 26 March 2004; received in revised form 21 September 2004; accepted 29 September 2004
Available online 22 February 2005

**Abstract**

Discretization of singular functions is an important component in many problems to which level set methods have been applied. We present two methods for constructing consistent approximations to Dirac delta measures concentrated on piecewise smooth curves or surfaces. Both methods are designed to be convenient for level set simulations and are introduced to replace the commonly used but inconsistent regularization technique that is solely based on a regularization parameter proportional to the mesh size. The first algorithm is based on a tensor product of regularized one-dimensional delta functions. It is independent of the irregularity relative to the grid. In the second method, the regularization is constructed from a one-dimensional regularization that is extended to multi-dimensions with a variable support depending on the orientation of the singularity relative to the computational grid. Convergence analysis and numerical results are given.


## 1. Introduction

In this paper, we study regularization methods for the Dirac delta function in the context of the level set method. This involves Dirac delta functions concentrated on a wide class of piecewise smooth, closed manifolds that are embedded through suitable continuous functions defined in Euclidean spaces of higher dimensions.

The level set method [8,10] is a highly successful computational technique for tracking the evolution of curves and surfaces. In connection to many applications of the level set method, the formulation includes a

* Corresponding author. Fax: +1 212 995 4121.
*E-mail address:* tornberg@cims.nyu.edu (A.-K. Tornberg).
[1] Research partially sponsored by NSF Grant DMS-9973341.
[2] Research partially sponsored by Swedish VR-Grant No. 222-2000-434.
[3] Research is supported in part by the National Science Foundation under agreement No. DMS-0111298.

0021-9991/$ - see front matter © 2005 Published by Elsevier Inc.
doi:10.1016/j.jcp.2004.09.018

Dirac delta measure supported on these curves or surfaces. In a typical level set method, the curves or surfaces are described implicitly as the zero level set of a continuous function, discretized on a uniform Cartesian grid. Singular Dirac delta functions are commonly regularized before they are represented on the computational grid. In the case of immiscible multiphase flow, regularization is applied to the singular surface tension forces supported on the interfaces separating the fluids [8,11]. Similarly, it has been used in other applications such as dendritic solidification and shape optimization problems [2], ranging from photonic crystals to active contours in image processing [8]. Typically, these applications include the computation of enforcing constraints defined on the surfaces using some variational approaches; see e.g. [3,18].

In light of a recent result [13] showing that the most common technique for regularization of the delta function in level set methods is inconsistent, and may lead to O(1) errors, the purpose of this paper is to develop consistent and effective regularizations that conveniently can be used in connection to level set methods.

There are a number of other useful methods for handling singularities in differential equations that are not based on regularization. Examples are the ghost fluid method and the immersed interface method, see e.g. [7,6]. Discussion of these types of techniques are beyond the scope of this paper.

Let $\Gamma \subset \mathbb{R}^d$ be a $d-1$ dimensional continuous and bounded surface and let $s$ be surface coordinates on $\Gamma$. Define $\delta(\Gamma, g, \mathbf{x}),\ \mathbf{x} \in \mathbb{R}^d$ as a delta function of variable strength supported on $\Gamma$ such that

$$I = \int_{\mathbb{R}^d} \delta(\Gamma, g, \mathbf{x}) f(\mathbf{x})\, \mathrm{d}\mathbf{x} = \int_{\Gamma} g(s) f(\mathbf{X}(s))\, \mathrm{d}s, \tag{1}$$

where $\mathbf{X}(s) \in \Gamma$.

Now assume that the space $\mathbb{R}^d$ is covered by a regular grid;

$$\begin{aligned} &\{\mathbf{x}_\mathbf{j}\}_{\mathbf{j}\in Z^d}, \quad \mathbf{x}_\mathbf{j} = (x_{j_1}^{(1)}, \ldots, x_{j_d}^{(d)}), \\ &x_{j_k}^{(k)} = x_0^{(k)} + j_k h_k, \quad j_k \in Z,\ \ k = 1, \ldots, d. \end{aligned} \tag{2}$$

Since we will consider fully general $\Gamma$ there is no restriction if we fix $x_0^{(k)}$ and we will for simplicity let $x_0^{(k)} = 0,\ k = 1, \ldots, d$ in the rest of the paper.

In the level set method, $\Gamma$ is defined by a level set function $\phi(\mathbf{x}) : \mathbb{R}^d \to \mathbb{R}$,

$$\Gamma = \{\mathbf{x} \mid \phi(\mathbf{x}) = 0\}.$$

We will first consider the case for which $\phi(\mathbf{x}) = d(\Gamma, \mathbf{x})$, where $d(\Gamma, \mathbf{x})$ is the signed distance function to $\Gamma$, and then proceed to study the extension to a non-distance function $\phi$. Let $\Gamma$ divide $\mathbb{R}^d$ into two disjoint subsets $\Omega_1$ and $\Omega_2$. Then

$$d(\Gamma, \mathbf{x}) = \begin{cases} \operatorname{dist}(\Gamma, \mathbf{x}), & \mathbf{x} \in \Omega_1, \\ -\operatorname{dist}(\Gamma, \mathbf{x}), & \mathbf{x} \in \Omega_2, \end{cases} \tag{3}$$

where $\operatorname{dist}(\Gamma, \mathbf{x})$ denotes the Euclidean distance from $\mathbf{x}$ to $\Gamma$, i.e., $\operatorname{dist}(\Gamma, \mathbf{x}) = \min_{\mathbf{y} \in \Gamma} |\mathbf{y} - \mathbf{x}|$.

The integral in Eq. (1) generally appears in the level set literature as

$$I = \int_{\mathbb{R}^d} \tilde{g}(\mathbf{x}) \delta(d(\Gamma, \mathbf{x})) f(\mathbf{x})\, \mathrm{d}\mathbf{x} = \int_{\mathbb{R}^d} \tilde{g}(\mathbf{x}) f(\mathbf{x}) \delta(\phi(\mathbf{x})) |\nabla \phi(\mathbf{x})|\, \mathrm{d}\mathbf{x}, \tag{4}$$

where $\tilde{g}$ is an extension of $g$ to $\mathbb{R}^d$, such that $\tilde{g}(\mathbf{X}(s)) = g(s)$. In this paper, we will not discuss the extension of $g$ to $\tilde{g}$. Methods for such extensions can, for example, be found in [8,10]. As Eq. (4) indicates, an extra scaling of $|\nabla\phi|$ is needed for the non-distance function $\phi$ in order to get the correct metric on $\Gamma$. We shall see later that this factor will play a role in our regularizations.

In later sections, different techniques will be used to regularize the $\delta$-function, and we will therefore use the more general notation

$$\delta(\Gamma, g, \mathbf{x}) = \tilde{g}(\mathbf{x})\delta(\Gamma, \mathbf{x}). \tag{5}$$

The delta function $\delta(\Gamma, \mathbf{x})$ will be replaced by a continuous function $\delta_{\boldsymbol{\varepsilon}}(\Gamma, \mathbf{x})$ of compact support. This regularized function will be discretized on the regular grid introduced in Eq. (2), and the integral over this function will be computed by evaluating a Riemann sum.

We define the discretization error as

$$E = \left| \left( \prod_{k=1}^{d} h_k \right) \sum_{\mathbf{j} \in Z^d} \delta_{\boldsymbol{\varepsilon}}(\Gamma, g, \mathbf{x}_\mathbf{j}) f(\mathbf{x}_\mathbf{j}) - \int_\Gamma g(s) f(\mathbf{X}(s))\, \mathrm{d}s \right| \tag{6}$$

following the definition in Eq. (1).

With $f \equiv g \equiv 1$, and $\Gamma$, a curve in $\mathbb{R}^2$, the $s$-coordinate being the arclength along $\Gamma$, the error $E$ is the error made in computing the length of the curve. More general, $g$-functions are common for singular source terms in differential equations, where $\delta(\Gamma, g, \mathbf{x})$ represents a physical force along an interface, such as an elastic force or a surface tension force. In Section 4.2, we shall see that the error term in Eq. (6) also plays an important role in the numerical approximation of differential equations.

Using the distance function $d(\Gamma, \mathbf{x})$ explicitly, for $g \equiv 1$ we can define

$$\delta_{\boldsymbol{\varepsilon}}(\Gamma, g, \mathbf{x}) = \delta_{\boldsymbol{\varepsilon}}(\Gamma, \mathbf{x}) = \delta_\varepsilon(d(\Gamma, \mathbf{x})), \tag{7}$$

where $\delta_\varepsilon$ is a one-dimensional regularization of the delta function and $2\varepsilon$ is the width of the support of $\delta_\varepsilon$. For this definition, it is possible to analyze the error in Eq. (6) by splitting it into an analytical and a numerical part, and consider those separately [12,14]. This analysis requires that $\delta_\varepsilon$ is sufficiently resolved on the underlying grid, and the result yields consistency and an optimal scaling of the regularization parameter $\varepsilon$ relative to the mesh size $h$, $\varepsilon \sim h^\alpha$, $0 < \alpha < 1$.

For a very narrow support, the $\delta_\varepsilon$ function is not sufficiently resolved to analyze the error by splitting it into these two parts. Instead, the error must be analyzed directly, taking into account discrete effects of the computational grid. In practice, this kind of approximations have been used with narrow support with $\varepsilon$ proportional to $h$, typically $\varepsilon = mh$, with $m = 1$, 2 or 3. This approach works well in one dimension, when the one-dimensional delta approximation obeys certain discrete moment conditions as discussed below. However, its extension to multi-dimension might lead to O(1) errors, as has been shown for a curve $\Gamma$ in $\mathbb{R}^2$ [13].

In one dimension, one can show [1] that the discretization error $E \leqslant Ch^q$ if the one-dimensional $\delta_\varepsilon$ function satisfies $q$ discrete moment conditions, i.e., if

$$h \sum_{j=-\infty}^{\infty} \delta_\varepsilon(x_j - \bar{x})(x_j - \bar{x})^r = \begin{cases} 1, & r = 0, \\ 0, & 1 \leqslant r < q \end{cases} \tag{8}$$

for all values of $\bar{x}$. If $\delta_\varepsilon$ satisfies $q$ moment conditions, we will say that it has a moment order $q$. The result $E \leqslant Ch^q$ carries nicely over to several dimensions if this multidimensional delta approximation is defined by the following product formula:

$$\delta_{\boldsymbol{\varepsilon}}(\Gamma, g, \mathbf{x}) = \int_\Gamma \prod_{k=1}^{d} \delta_{\varepsilon_k}(x^{(k)} - X^{(k)}(s)) g(s)\, \mathrm{d}s \tag{9}$$

in which $\delta_{\varepsilon_k}$ corresponds to the one-dimensional regularized $\delta$ function, $\mathbf{x} = (x^{(1)}, \ldots, x^{(d)})$, $\mathbf{X}(s) = (X^{(1)}(s), \ldots, X^{(d)}(s))$ is a parameterization of $\Gamma$ and $\boldsymbol{\varepsilon} = m(h_1, \ldots, h_d)$. The grid sizes $h_1, \ldots, h_d$ refers to the regular grid introduced in Eq. (2). This was proved in [13]. This product formula is often used in methods, where $\Gamma$ is explicitly defined, for example in the immersed boundary method of Peskin [9].

When $\Gamma$ is not explicitly defined, the product formula is not a convenient definition. In level set methods, it is more natural to define $\delta_{\boldsymbol{\varepsilon}}(\Gamma, \mathbf{x}) = \delta_\varepsilon(d(\Gamma, \mathbf{x}))$, or with a level set function $\phi$ that is not a distance func-

tion, including an appropriate scaling, as will be discussed in Section 5.1. However, as noted above, this does not work well with the choice of constant $\varepsilon$, proportional to the grid size, $\varepsilon = mh$, $h = h_1 = \cdots = h_d$, which has been the most common choice in practice. This is further discussed in Section 2.

In this paper, we derive two techniques for regularizing the delta function when $\Gamma$ is defined implicitly the distance function, $d(\Gamma, \mathbf{x})$. These two techniques are then conveniently extended to the case of a non-distance level set function. In both cases, the resulting regularized delta functions depend only on the level set function but not the underlying grid. In Section 3.1, we introduce an approximation of the product rule in Eq. (9), that can be defined using the distance function to $\Gamma$, $d(\Gamma, \mathbf{x})$, together with the gradient of this function. We prove that this regularization gives first-order convergence for continuous and piecewise $C^2$ curves $\Gamma$ in $\mathbb{R}^2$. We conjecture that the regularization is also second-order accurate in the grid size $h$ for smooth $\Gamma$. Numerical tests confirm this hypothesis.

The second approach, introduced in Section 3.2, is the one most simple to apply. It uses the same definition as in Eq. (7), but instead of a constant $\varepsilon = \varepsilon_0$, it uses a variable support of the regularized delta function, such that $\varepsilon = \varepsilon(\nabla d, \varepsilon_0)$. We prove that for a constant $f$ in Eq. (6), the error $E = 0$ for a line $\Gamma$ in $\mathbb{R}^2$ with a rational slope on a large class of grids, and $O(h)$ for more general settings. Numerical tests indicate that the method is first-order accurate in the grid size $h$ also for a general $\Gamma$.

Numerical results for these two methods, both in connection to quadrature and to the numerical solution of a partial differential equation with a singular source term, are presented in Section 4. In Section 5, we discuss the generalization of the approaches presented in Section 3 for the following cases: (1) non-distance level set functions, (2) regularization of characteristic functions, (3) $\Gamma$ as a surface in three dimensions. We show numerical results for each of the cases listed above, and finally discuss the possible extension to manifolds of higher codimension.

## 2. Discrete regularization of singularities

In this section, we begin by discussing the regularization of a one-dimensional $\delta$-function, introducing the essential discrete moment conditions. We continue by discussing the extension to several dimensions and address the inconsistency of the extension using the distance function as in Eq. (7), with the regularization parameter proportional to the grid size.

Let us start this discussion with the definition of the discrete moment conditions.

**Definition 2.1.** A function $\delta_\varepsilon(x) \in Q^q$ if $\delta_\varepsilon$ has compact support in $[-\varepsilon, \varepsilon]$, $\varepsilon = mh$, $m > 0$ and

$$M_r(\delta_\varepsilon, \bar{x}, h) = h \sum_{j=-\infty}^{\infty} \delta_\varepsilon(x_j - \bar{x})(x_j - \bar{x})^r = \begin{cases} 1, & r = 0, \\ 0, & 1 \leqslant r < q \end{cases} \tag{10}$$

for any $\bar{x} \in \mathbb{R}$, where $x_j = jh$, $h > 0$, $j \in Z$.

The first moment condition, for $r = 0$, ensures that the mass of the delta function is identically 1, independent on shifts in the grid. The higher moment conditions are useful when the delta function is multiplied by a non-constant function, as we will see in the proposition below. The following result was given in [1].

**Proposition 1.** *Suppose that $\delta_\varepsilon \in Q^q$, $q > 0$ as in Definition 2.1, $f(x) \in C^q(\mathbb{R})$, and that all derivatives of $f$ are bounded, then*

$$E = \left| h \sum_{j=-\infty}^{\infty} \delta_\varepsilon(x_j - \bar{x}) f(x_j) - f(\bar{x}) \right| \leqslant Ch^q,$$

*and $E = 0$ if $f$ is constant.*

From this proposition, we see that the numerical accuracy is determined by the moment order of the delta function approximation. The discretization error $E$ can be interpreted as the error made when integrating by the trapezoidal rule, with $\bar{x}$ away from the boundary. It can also be regarded as the error in interpolating $f$ at $\bar{x}$ from the grid values of $f$, the choice of $\delta_\varepsilon$ determining the interpolation weights.

In [13], it was shown that such an $\delta_\varepsilon \in Q^q$ exists if and only if $2\varepsilon \geqslant qh$. The most compact $\delta_\varepsilon$ approximation that obeys $q$ moment conditions may however not be continuous. In computations, it is most practical to deal with continuous $\delta_\varepsilon$ functions, and we define approximate delta functions $\delta_\varepsilon$ on the form

$$\delta_\varepsilon(x) = \begin{cases} \frac{1}{\varepsilon}\psi(x/\varepsilon), & |x| \leqslant \varepsilon = mh, \\ 0 & |x| > \varepsilon = mh, \end{cases} \tag{11}$$

where $\delta_\varepsilon \in C(\mathbb{R})$, i.e., $\psi(-1) = \psi(1) = 0$. With this notation, the linear hat function $\delta_\varepsilon^L$ is defined as above with

$$\psi^L(\xi) = 1 - |\xi| \tag{12}$$

and the much used cosine function $\delta_\varepsilon^{\cos}$ with,

$$\psi^{\cos}(\xi) = \tfrac{1}{2}(1 + \cos(\pi\xi)). \tag{13}$$

For both these approximations, the mass condition, i.e., the moment condition for $r = 0$ is fulfilled for $m \geqslant 1$ integer with $\varepsilon = mh$ for the linear hat function, and $\varepsilon = (m + 1)/2h$ for the cosine function. The moment condition for $r = 1$ is not satisfied for the cosine approximation, and hence it is of moment order one. The linear hat functions are of moment order two. From Proposition 1, we have that the error is of $O(h)$ for the cosine function, and $O(h^2)$ for the linear hat function. It is possible to construct approximations of higher moment order. In [13], a $\delta_\varepsilon$ function based on a cubic polynomial with $\varepsilon = 2h$ with moment order four was introduced, and approximations with even higher moment orders can be found in [17].

As mentioned in Section 1, one approach to create a regularization of a $\delta$-function with support on a multidimensional $\Gamma$ such as a curve in $\mathbb{R}^2$ or $\mathbb{R}^3$ or a surface in $\mathbb{R}^3$, is to use the product formula in Eq. (9). In this manner, a one-dimensional $\delta_\varepsilon$ function is used in each coordinate direction, and in [13], Tornberg and Engquist proved the following theorem.

**Theorem 1.** *Suppose that $\delta_\varepsilon \in Q^q$, $q > 0$, as in Definition 2.1; $g \in C^r(\mathbb{R}^d)$ and $f \in C^r(\mathbb{R}^d)$, $r \geqslant q$. Then for any rectifiable curve $\Gamma$ and $\delta_\varepsilon(\Gamma, g, \mathbf{x})$ as defined in Eq. (9) based on $\delta_\varepsilon$, it holds that*

$$E = \left| \left( \prod_{k=1}^{d} h_k \right) \sum_{\mathbf{j} \in Z^d} \delta_\varepsilon(\Gamma, g, \mathbf{x_j}) f(\mathbf{x_j}) - \int_\Gamma g(S) f(\mathbf{X}(S))\, \mathrm{d}S \right| \leqslant Ch^q \tag{14}$$

*with $h = \max_{1 \leqslant k \leqslant d} h_k$ and $E = 0$ for constant $f$.*

The accuracy of delta function approximations defined by this product formula will hence be determined by the number of discrete moments that the one-dimensional $\delta_\varepsilon$ function obeys, and it is therefore simple to construct regularizations of desired accuracy. The product definition is however not convenient for defining the $\delta_\varepsilon$-function when $\Gamma$ is defined implicitly through a distance function, since it requires the explicit parameterization of $\Gamma$.

As discussed in Section 1, a common technique for extending the regularized one-dimensional delta function to several dimensions in connection to the level set method is to define

$$\delta_\varepsilon(\Gamma, \mathbf{x}) = \delta_\varepsilon(d(\Gamma, \mathbf{x})). \tag{15}$$

The choice of the support in practical level set simulations has mainly been $\varepsilon = h$ or $\varepsilon = 2h$, for discretization on regular grids [8,10]. In [13], it was shown that such a choice may result in an $O(1)$ error, by using an

example of a curve $\Gamma \in \mathbb{R}^2$, that is a straight line at an angle of 45° to the $x^{(1)}$-axis; $\Gamma = \{\mathbf{x}, x^{(1)} = x^{(2)}, 0 \leqslant x^{(1)} < \bar{S}/\sqrt{2}\}$. For completeness, we briefly review this derivation.

Considering the calculation of the length $|\Gamma|$,

$$|\Gamma| = \bar{S} = \int_{\mathbb{R}^2} \delta(\Gamma, \mathbf{x})\, \mathrm{d}\mathbf{x} \tag{16}$$

computed using a $\delta_\varepsilon$ approximation on a regular grid,

$$\bar{S}_h = h^2 \sum_{\mathbf{j} \in Z^2} \delta_\varepsilon(d(\Gamma, \mathbf{x}_\mathbf{j})), \quad x_{j_k}^{(k)} = j_k h, \;\; j_k \in Z, \;\; k = 1, 2, \tag{17}$$

it was shown that, with $\delta_\varepsilon = \delta_h^L$, the narrow linear hat function, this yields

$$\bar{S}_h = \frac{3 - \sqrt{2}}{\sqrt{2}} \bar{S} + \mathrm{O}(h),$$

which results in a relative error $(|\bar{S}_h - \bar{S}|/\bar{S})$ of over 12% as $h \to 0$. Repeating the exercise for the wider piecewise linear hat function with $\varepsilon = 2h$ the result is

$$\bar{S}_h = \tfrac{1}{4}(5\sqrt{2} - 3)\bar{S} + \mathrm{O}(h),$$

which yields a relative error of 1.8% as $h \to 0$.

Numerical tests were conducted to illustrate this fact. Here, let $\Gamma$ be defined as two parallel lines of length $L$ at a normal distance $2a$, joined at both ends by a half circle of radius $a$. The angle of the lines to the $x$-axis is $\theta = \pi/4$. A sketch of $\Gamma$ is plotted in Fig. 1. The total length of $\Gamma$ is $\bar{S} = 2L + 2\pi a$.

We again define the relative error in the computation of the length of $\Gamma$ as $E = |\bar{S}_h - \bar{S}|/\bar{S}$, with $\bar{S}$ and $\bar{S}_h$ as defined in Eqs. (16) and (17). In Fig. 2, the relative error $E$ is plotted versus $1/h$, where $h$ is the grid size, for different values of $L$ and $a$. In the left plot, we display the results for the narrow piecewise linear hat function, $\delta_h^L$. In this plot, we can clearly see that there is no convergence as $h$ is decreased. As $a/L$ decreases, the error from the straight lines dominates more and more, and for $a = 0.03\sqrt{2},\ L = 4.0$ (line marked with $\diamond$) the relative error is close to the 12% as predicted for the straight lines. In the right plot, the results are plotted for the wider hat function, $\delta_{2h}^L$. The errors are smaller in this case, but also here, we have no convergence as $h$ is decreased, and for $a = 0.03\sqrt{2},\ L = 4.0$ (line marked with $\diamond$) we again approach the predicted relative error for the straight line, in this case 1.78%.

Even though the size of the O(1) error may vary for different delta approximations in this example, the order of the error does not depend on the specific choice of the delta function approximation $\delta_\varepsilon$, that is used to define $\delta_\varepsilon(d(\Gamma, \mathbf{x}))$. The accuracy of the one-dimensional regularizations, as well as the multidimensional extension by the product rule, relies on the discrete moment conditions. For the delta approximations with

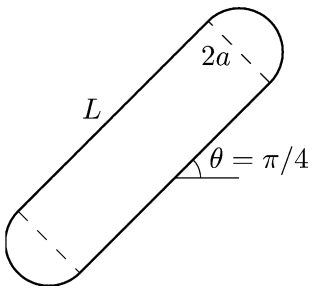


Fig. 1. Sketch of curve $\Gamma$.

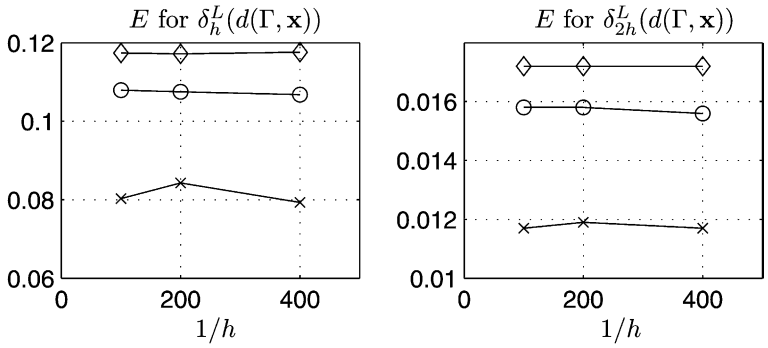


Fig. 2. The relative error $E = |\bar{S}_h - \bar{S}|/\bar{S}$ plotted versus $1/h$, with $\bar{S}$ and $\bar{S}_h$ defined as in Eqs. (16) and (17). The delta function approximation is based on the linear hat function, in the left figure with $\varepsilon = h$, in the right with $\varepsilon = 2h$. $\Gamma$ as shown in Fig. 1, with $L = 2.0$, $a = 0.24\sqrt{2}$ (×), $L = 2.0$, $a = 0.06\sqrt{2}$ (○), $L = 4.0$, $a = 0.03\sqrt{2}$ (◇).

compact support that we are studying here, the mass condition and possibly higher moment conditions are fulfilled for $\varepsilon = mh$, where $m$ is an integer, and possibly also for $2\varepsilon = \beta h$, with $\beta$ an integer. However, if $\varepsilon$ does not relate to $h$ in the required way, even the mass condition is in general no longer fulfilled, leading to an O(1)-error, as was shown in [14]. Similarly in this two-dimensional case, with $\Gamma$ at some arbitrary angle to the grid lines, no such discrete sums will in general evaluate correctly, and hence we obtain an O(1) error.

This choice of $\Gamma$ shows a special case with large errors. All local errors in the linear part of $\Gamma$ have the same sign and no cancellation of errors occur. This case was selected since it clearly illustrates the substantial O(1) errors that do exist for this approach.

## 3. New discrete regularization techniques

In this section, we introduce two new consistent techniques for regularizing a delta function based on the distance function to $\Gamma$ and its gradient.

### 3.1. Approximate product formula

From Theorem 1, we know that when a multidimensional delta function approximation is defined by the product rule in Eq. (9), we can control the accuracy by the design of the one-dimensional $\delta$-function approximation. The product rule does however require an explicit parameterization of $\Gamma$, and is therefore not convenient for defining the $\delta_\varepsilon$-function when $\Gamma$ is defined implicitly through a distance function. It is however possible to construct an approximation to this product rule, where we only make use of the distance function and its gradient.

Consider a curve $\Gamma$ in two dimensions. As defined in Eq. (3), we use $d(\Gamma, \mathbf{x})$ to denote the signed distance function that embeds $\Gamma$, and we assume that $\varepsilon = \varepsilon_1 = \varepsilon_2$. An approximation to the product definition of $\delta_\varepsilon$ in a point $\mathbf{x}$ can be computed by

$$\tilde{\delta}_\varepsilon(\Gamma,\mathbf{x}) = \int_\Gamma \delta_\varepsilon^L(x - \bar{X}(\mathbf{x},s))\delta_\varepsilon^L(y - \bar{Y}(\mathbf{x},s))\,\mathrm{d}s, \tag{18}$$

where $(\bar{X}(\mathbf{x},s), \bar{Y}(\mathbf{x},s))$, $s \in \mathbb{R}$ is the tangent line to $\bar{\mathbf{x}} \in \Gamma$, the closest point on $\Gamma$ to $\mathbf{x}$. The one-dimensional $\delta_\varepsilon$ function is the linear hat function. Due to the compact support of the one-dimensional $\delta_\varepsilon$-function, this integrand is non-zero only in the box $[x-\varepsilon, x+\varepsilon] \times [y-\varepsilon, y+\varepsilon]$, and within this box, the tangent line $\bar{\mathbf{X}}(\mathbf{x},s) = (\bar{X}(\mathbf{x},s), \bar{Y}(\mathbf{x},s))$ will be close to $\Gamma$, see Fig. 3.

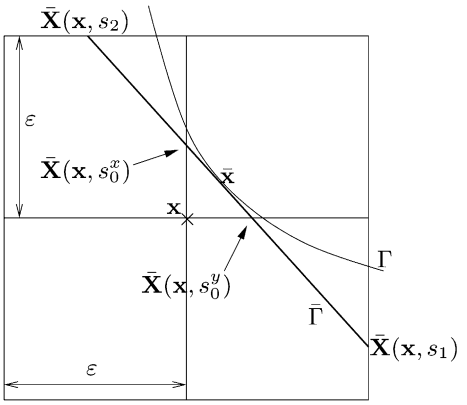


Fig. 3. The integrand in Eq. (18), defining $\tilde{\delta}_\varepsilon(\Gamma, \mathbf{x})$, $\mathbf{x} = (x, y)$, is non-zero only in the box $[x - \varepsilon, x + \varepsilon] \times [y - \varepsilon, y + \varepsilon]$. Within this box, $\Gamma$ is approximated by the tangent line $\bar{\Gamma}$. To evaluate the integral, intersections of $\bar{\Gamma}$ with the grid lines must be computed.

Hence, to evaluate the integral in Eq. (18), we need to define the straight line $(\bar{X}(\mathbf{x}, s), \bar{Y}(\mathbf{x}, s))$ and find how it cuts through this box. Define this line by

$$\bar{\Gamma}(\mathbf{x}, s) := \begin{pmatrix} \bar{X}(\mathbf{x}, s) \\ \bar{Y}(\mathbf{x}, s) \end{pmatrix} = \mathbf{x} - \left[ d(\Gamma, \mathbf{x}) \begin{pmatrix} \cos\theta \\ \sin\theta \end{pmatrix} + s \begin{pmatrix} -\sin\theta \\ \cos\theta \end{pmatrix} \right],$$

where $s$ is the arclength and $\theta$ is the angle of the normal vector $\mathbf{n}_{\bar{\Gamma}}$ of $\bar{\Gamma}$ to the $x$-axis, with $\mathbf{n}_{\bar{\Gamma}}$ defined to point into the region where $d(\Gamma,\mathbf{x}) > 0$.

Using the definition of the linear hat function, the integral in Eq. (18) is defined as

$$\begin{aligned} \tilde{\delta}_\varepsilon(\Gamma, \mathbf{x}) &= \int_{s_1}^{s_2} \frac{1}{\varepsilon} \left( 1 - \frac{1}{\varepsilon} |d\cos\theta - s\sin\theta| \right) \frac{1}{\varepsilon} \left( 1 - \frac{1}{\varepsilon} |d\sin\theta + s\cos\theta| \right) \mathrm{d}s \\ &= \frac{1}{\varepsilon} \int_{s_1/\varepsilon}^{s_2/\varepsilon} \left( 1 - \left| \frac{d}{\varepsilon}\cos\theta - \tilde{s}\sin\theta \right| \right) \left( 1 - \left| \frac{d}{\varepsilon}\sin\theta + \tilde{s}\cos\theta \right| \right) \mathrm{d}\tilde{s}, \end{aligned} \tag{19}$$

where $d = d(\Gamma, \mathbf{x})$ and $s = s_1$, $s = s_2$ are the $s$-values at which $(\bar{X}(s), \bar{Y}(s))$ intersects the boundaries of the box $[x - \varepsilon, x + \varepsilon] \times [y - \varepsilon, y + \varepsilon]$.

The evaluation of the integrals will depend on the sign of the arguments within the two absolute signs. The line integral can conveniently be split into different pieces, such that each lies within one quadrant of the box $[x - \varepsilon, x + \varepsilon] \times [y - \varepsilon, y + \varepsilon]$. To define these segments, in addition to $s_1$ and $s_2$ we need to define (if applicable), $s = s_0^x$ such that $(\bar{X}(s_0^x), \bar{Y}(s_0^x)) = (x, \bar{Y}(s_0^x))$, and $s = s_0^y$ such that $(\bar{X}(s_0^y), \bar{Y}(s_0^y)) = (\bar{X}(s_0^y), y)$, see Fig. 3. This requires finding intersection of straight lines.

Since the integrand is an even function, we can restrict $\theta$ to $\theta \in [0, \pi/2]$ and compute it by $\theta = \arctan(|d_y/d_x|)$, i.e., using the components of $\nabla d$. Let $K = [s_1, s_2]$. Then, $\tilde{\delta}_\varepsilon(\Gamma, \mathbf{x})$, as defined in Eq. (18) and subsequently in Eq. (19) can be evaluated as

$$\tilde{\delta}_\varepsilon(\Gamma, \mathbf{x}) = \begin{cases} I^\varepsilon_{+,+}(s_1, s_2, d, \theta) & \text{if } s_0^x, s_0^y \notin K, \\ I^\varepsilon_{+,+}(s_1, s_0^x, d, \theta) + I^\varepsilon_{-,+}(s_0^x, s_2, d, \theta) & \text{if } s_0^x \in K \text{ and } s_0^y \notin K, \\ I^\varepsilon_{+,-}(s_1, s_0^y, d, \theta) + I^\varepsilon_{+,+}(s_0^y, s_2, d, \theta) & \text{if } s_0^x \notin K \text{ and } s_0^y \in K, \\ I^\varepsilon_{+,-}(s_1, s_0^y, d, \theta) + I^\varepsilon_{+,+}(s_0^y, s_0^x, d, \theta) + I^\varepsilon_{-,+}(s_0^x, s_2, d, \theta) & \text{if } s_0^x, s_0^y \in K, \end{cases}$$

where $d = d(\Gamma, \mathbf{x})$. Using $c_1 = \pm 1$ and $c_2 = \pm 1$ to represent the signs in the subscript, the integrals above evaluate as $I^\varepsilon_{c_1,c_2}(s_a, s_b, d, \theta) = I_{c_1,c_2}(s_a/\varepsilon, s_b/\varepsilon, d/\varepsilon, \theta)/\varepsilon$, where

$$I_{c_1,c_2}(a,b;\tilde{d},\theta) = \int_a^b \big(1 + c_1\big(\tilde{d}\cos\theta - \alpha\sin\theta\big)\big)\big(1 + c_2\big(\tilde{d}\sin\theta + \alpha\cos\theta\big)\big)\,\mathrm{d}\alpha$$
$$= \frac{1}{2}c_1c_2\sin 2\theta[\alpha]_a^b\tilde{d}^2 + \left(\frac{1}{2}c_1c_2\cos 2\theta[\alpha^2]_a^b + (c_1\cos\theta + c_2\sin\theta)[\alpha]_a^b\right)\tilde{d}$$
$$+ \left(-\frac{1}{6}c_1c_2\sin 2\theta[\alpha^3]_a^b + \frac{1}{2}(-c_1\sin\theta + c_2\cos\theta)[\alpha^2]_a^b + [\alpha]_a^b\right). \tag{20}$$

A derivation of the parameters $s_1, s_2, s_0^x,$ and $s_0^y$ using $d(\Gamma, \mathbf{x})$ and its gradient is presented in Appendix A.

In the following theorem, we show that our approximation is at least first-order accurate.

**Theorem 2.** *Let $\tilde{\delta}_\varepsilon(\Gamma,\mathbf{x})$ denote the approximate delta function as defined in Eq. (18) with $\varepsilon = mh$, $m$ integer. Then there is a constant $C \geqslant 0$ such that*

$$E = \left|h^2\sum_{\mathbf{j}\in\mathbb{Z}^2}\tilde{\delta}_\varepsilon(\Gamma,\mathbf{x}_\mathbf{j})f(\mathbf{x}_\mathbf{j}) - \int_\Gamma f(X(s))\,\mathrm{d}s\right| \leqslant Ch,$$

*assuming that $\Gamma \subset \mathbb{R}^2$ is piecewise $C^2$ and of bounded length.*

**Proof.** Let $\delta_{\boldsymbol{\varepsilon}}^L(\Gamma,\mathbf{x})$ be the delta approximation defined by the product rule in Eq. (9), as based on the one-dimensional hat function $\delta_{\varepsilon_k}^L$, with $\varepsilon_1 = \varepsilon_2 = \varepsilon = mh$, where $h^{(1)} = h^{(2)} = h$, and with $g \equiv 1$. Then, from Theorem 1, we have that

$$\left|h^2\sum_{\mathbf{j}\in\mathbb{Z}^2}\delta_{\boldsymbol{\varepsilon}}^L(\Gamma,\mathbf{x}_\mathbf{j})f(\mathbf{x}_\mathbf{j}) - \int_\Gamma f(X(s))\,\mathrm{d}s\right| \leqslant D_1h^2 \tag{21}$$

since the hat function is of moment order two ($\delta_\varepsilon^L \in Q^2$).

Let

$$I = h^2\sum_{\mathbf{j}\in\mathbb{Z}^2}\delta_{\boldsymbol{\varepsilon}}^L(\Gamma,\mathbf{x}_\mathbf{j})f(\mathbf{x}_\mathbf{j}), \quad \tilde{I} = h^2\sum_{\mathbf{j}\in\mathbb{Z}^2}\tilde{\delta}_\varepsilon(\Gamma,\mathbf{x}_\mathbf{j})f(\mathbf{x}_\mathbf{j}).$$

With this, we have

$$E = \left|\tilde{I} - \int_\Gamma f(X(s))\,\mathrm{d}s\right| \leqslant |\tilde{I} - I| + \left|I - \int_\Gamma f(X(s))\,\mathrm{d}s\right|, \tag{22}$$

where the second part is bounded by $D_1h^2$ as given in Eq. (21). Now, we want to show that $|\tilde{I} - I| \leqslant D_2h$, for some constant $D_2$.

Define $J$ to be the index set such that $\mathbf{j} = (j_1, j_2) \in J$ if and only if $\min_s(\max(|x_{j_1} - X(s)|,\ |y_{j_2} - Y(s)|)) \leqslant mh$. The number of indices in $J$ : $|J| \leqslant C_1h^{-1}$ since $\Gamma$ is bounded. We have that

$$|I - \tilde{I}| \leqslant h^2\sum_{\mathbf{j}\in J}|\delta_{\boldsymbol{\varepsilon}}^L(\Gamma,\mathbf{x}_\mathbf{j}) - \tilde{\delta}_\varepsilon(\Gamma,\mathbf{x}_\mathbf{j})||f(\mathbf{x}_\mathbf{j})| = \Upsilon_A + \Upsilon_B, \tag{23}$$

where $\Upsilon_A$ is the sum over the index set $J_A$, where $J_A$ contains all indices of points near (Euclidean distance smaller than $mh\sqrt{2}$) a point where $\Gamma$ is not $C^1$, and $\Upsilon_B$ is the sum over the remaining terms.

There are finitely many such points, $|J_A| \leqslant C_2$, which implies

$$\Upsilon_A \leqslant h^2C_2C_3h^{-1}\|f\|_{L^\infty} = D_3h$$

since $C_3h^{-1}$ is the bound for the point values of $\delta_\varepsilon^L$ and $\tilde{\delta}_\varepsilon$. For the rest of the sum (denoted by $_B$ above), $\Gamma$ is $C^1$, and we have

$$\Upsilon_B = h^2 \sum_{\mathbf{j}\in J_B} |\delta_\varepsilon^L(\Gamma,\mathbf{x_j}) - \tilde{\delta}_\varepsilon(\Gamma,\mathbf{x_j})||f(\mathbf{x_j})| \leqslant h^2 C_1 h^{-1} \max_{\mathbf{j}\in J_B} |\delta_\varepsilon^L(\Gamma,\mathbf{x_j}) - \tilde{\delta}_\varepsilon(\Gamma,\mathbf{x_j})| \left\|f(\mathbf{x_j})\right\|_{L^\infty} \leqslant hC_4\Upsilon_D,$$

where $C_4 = C_1\|f\|_{L^2}$ and $\Upsilon_D = \max_{\mathbf{j}\in J_B}|\delta_\varepsilon^L(\Gamma,\mathbf{x_j}) - \tilde{\delta}_\varepsilon(\Gamma,\mathbf{x_j})|$. Defining $\Gamma = (X(s), Y(s))$, and the tangent line $\bar{\Gamma}(\mathbf{x},s) = (\bar{X}(\mathbf{x},s), \bar{Y}(\mathbf{x},s))$, we can write

$$\Upsilon_D = \max_{\mathbf{j}\in J_B} \left| \int_\Gamma \delta_\varepsilon^L(x_{j_1} - X(s))\delta_\varepsilon^L(y_{j_2} - Y(s))\,\mathrm{d}s - \int_{\bar{\Gamma}} \delta_\varepsilon^L(x_{j_2} - \bar{X}(\mathbf{x_j},s))\delta_\varepsilon^L(y_{j_2} - \bar{Y}(\mathbf{x_j},s))\,\mathrm{d}s \right|,$$

where we have used the definitions of $\delta_\varepsilon^L(\Gamma,\mathbf{x_j})$ (Eq. (9)) and $\tilde{\delta}_\varepsilon(\Gamma,\mathbf{x_j})$ (Eq. (18)). Define the arclength variable $s$ in the different integrals such that $\bar{\mathbf{x}}$, the closest point on $\Gamma$ to $\mathbf{x_j}$, corresponds to $s = 0$ both on $\Gamma$ and $\tilde{\Gamma}$. Let $s_1, s_2$ and $\tilde{s}_1, \tilde{s}_2$ denote the end points of the support of $\delta_\varepsilon^L(x_{j_1} - X(s))\delta_\varepsilon^L(y_{j_2} - Y(s))$ and $\delta_\varepsilon^L(x_{j_1} - \bar{X}(\mathbf{x_j},s))$ $\delta_\varepsilon^L(y_{j_2} - \bar{Y}(\mathbf{x_j},s))$ along $\Gamma$ and $\tilde{\Gamma}$, respectively. Then we have

$$\Upsilon_D \leqslant \int_{\min(s_1,\tilde{s}_1)}^{\max(s_2,\tilde{s}_2)} \left| \delta_\varepsilon^L(x_{j_1} - X(s))\delta_\varepsilon^L(y_{j_2} - Y(s)) - \delta_\varepsilon^L(x_{j_1} - \bar{X}(\mathbf{x_j},s))\delta_\varepsilon^L(y_{j_2} - \bar{Y}(\mathbf{x_j},s)) \right| \mathrm{d}s.$$

On each side, the integral over one of the curves is extended outside its original definition, but since such an extended part falls outside of the support of the delta function, it yields no contribution, and hence, does not change the value of the integral.

Now, let us write

$$\delta_\varepsilon^L(x_{j_1} - \bar{X}(\mathbf{x_j},s)) = \delta_\varepsilon^L(x_{j_1} - X(s)) + \Upsilon_E,$$

and estimate the size of $|\Upsilon_E|$. We have that $|X(s) - \bar{X}(\mathbf{x_j},s)| \leqslant C_5h^2$ from the bounded curvature of $\Gamma$, and $|(\delta_\varepsilon^L)'| \leqslant C_6h^{-2}$. Using this, it follows that $|\Upsilon_E| \leqslant C_5h^2 \cdot C_6h^{-2} = C_5C_6$. $\Upsilon_E$ is simply the remainder term in a one term Taylor expansion of $\delta_\varepsilon^L$.

Similarly for

$$\delta_\varepsilon^L(y_{j_2} - \bar{Y}(\mathbf{x_j},s)) = \delta_\varepsilon^L(y_{j_2} - Y(s)) + \Upsilon_F,$$

it follows that $|\Upsilon_F| \leqslant C_5C_6$. Returning to the estimate for $\Upsilon_D$, we now have

$$\begin{aligned}\Upsilon_D &\leqslant \int_{\min(s_1,\tilde{s}_1)}^{\max(s_2,\tilde{s}_2)} \left( |\delta_\varepsilon^L(x_{j_1} - X(s))||\Upsilon_F| + \delta_\varepsilon^L(y_{j_2} - Y(s))||\Upsilon_E| + |\Upsilon_E||\Upsilon_F| \right) \mathrm{d}s \\ &\leqslant (\max(s_2,\tilde{s}_2) - \min(s_1,\tilde{s}_1)) \cdot \left( \left\|\delta_\varepsilon^L\right\|_{L^\infty} \cdot C_5C_6 + C_5^2C_6^2 \right).\end{aligned}$$

This implies that $_D$ is bounded by a constant, $\Upsilon_D \leqslant C_7$, and so $_B \leqslant C_4C_7h$. From before, we had that $\Upsilon_A$ is bounded by $D_3h$, and so from Eq. (23), $|I - \tilde{I}| \leqslant D_2h$, for $D_2 = D_3 + C_4C_7$. This yields $E \leqslant Ch$, from Eq. (22). □

The tangent line $\bar{\Gamma}(\mathbf{x},s)$ used to define $\tilde{\delta}_\varepsilon(\Gamma,\mathbf{x})$ depends on $\mathbf{x}$, the point in which $\tilde{\delta}_\varepsilon$ is to be evaluated. Hence, there is no global representation of $\bar{\Gamma}$, and a potential proof of more than first-order convergence will be more complex and include the effect of cancellations over a large segment of $\Gamma$.

Now, assume that we instead define $\bar{\Gamma}$ as the piecewise linear curve passing through all intersection points of $\Gamma$ and the grid lines, and define $\delta_\varepsilon^L(\bar{\Gamma},\mathbf{x})$ for this $\bar{\Gamma}$ using the product rule in Eq. (18), based on the one-dimensional hat-function. This is the usual definition of a delta approximation, based on the product rule, but with respect to $\bar{\Gamma}$ instead of $\Gamma$. From Theorem 1, we then have,

$$\left| h^2 \sum_{\mathbf{j}\in\mathbb{Z}^2} \delta_\varepsilon^L(\bar{\Gamma},\mathbf{x_j}) f(\mathbf{x_j}) - \int_{\bar{\Gamma}} f(\bar{X}(s),\bar{Y}(s))\,\mathrm{d}s \right| \leqslant C_1h^2, \tag{24}$$

where the integral over $f$ now is along $\bar{\Gamma}$. Furthermore, for a sufficiently regular $\Gamma$ we can show that

$$\left| \int_{\bar{\Gamma}} f(\bar{X}(s), \bar{Y}(s)) \, \mathrm{d}s - \int_{\Gamma} f(X(s), Y(s)) \, \mathrm{d}s \right| \leqslant C_2 h^2,$$

where $C_2$ depends on the curvature bound of $\Gamma$. For $f \equiv 1$, this is simply the difference in length between $\Gamma$ and $\bar{\Gamma}$. In total this yields,

$$\left| h^2 \sum_{\mathbf{j} \in \mathbb{Z}^2} \delta_{\varepsilon}^{L}(\bar{\Gamma}, \mathbf{x}_{\mathbf{j}}) f(\mathbf{x}_{\mathbf{j}}) - \int_{\Gamma} f(X(s), Y(s)) \, \mathrm{d}s \right| \leqslant (C_1 + C_2) h^2. \tag{25}$$

For this definition, we can hence show second-order convergence. This definition however requires explicit computation of intersections of the zero level set and the grid lines. One has to recompute line segments in order to define the delta function whenever the underlying grid is changed.

This is certainly possible, but we do not see any advantage over the one we propose through Eq. (18), since the latter is solely based on distance functions, and can be used directly to different grids and even curves that cannot be represented by conventional level set methods.

### 3.2. Variable regularization parameter

For the product rule discussed in the previous section, the effective support size of the approximate delta function varies according to how $\Gamma$ cuts through the given Cartesian grid. As measured in normal distance from $\Gamma$, the approximate delta function assumes the widest support when $\Gamma$ is diagonal to the grid, and the smallest when $\Gamma$ is parallel to the grid lines. In this section, we exploit this observation and derive a special scaling of the support according to the grid orientation of $\Gamma$.

We will derive a scaling for $\varepsilon$ that depends on the gradient of the signed distance function $d(\Gamma,\mathbf{x})$, such that $\varepsilon = \varepsilon(\nabla d, \varepsilon_0)$, where $\varepsilon_0$ is constant. The regularized delta function in any point $\mathbf{x}$ is then simply evaluated as $\delta_{\varepsilon(\nabla d,\varepsilon_0)}(d(\Gamma,\mathbf{x}))$, as based on a one-dimensional $\delta_\varepsilon$ function. The method will apply to general curves $\Gamma$, but in order to derive $\varepsilon(\nabla d,\varepsilon_0)$, we begin by studying a case where $\Gamma$ is a straight line. Let $\Gamma_{p,\,q}$ denote the line $(ps, qs),\ s \in \mathbb{R}$, which is in the direction of the unit vector $(p,q)/\sqrt{p^2+q^2}$. Assume furthermore that $p$ and $q$ denote two relative prime positive integers, i.e., two integers that have no common denominator other than 1. We will show that with a choice of

$$\varepsilon = \tilde{\varepsilon}(p,q) = \frac{p+q}{\sqrt{p^2+q^2}}$$

an exact summation property holds.

With this choice of $\tilde{\varepsilon}(p,q)$, the region of support of the delta function $\delta_{\tilde{\varepsilon}(p,q)}(d(\Gamma_{p,q},\mathbf{x}))$, for the segment of $\Gamma_{p,\,q} = (ps,\, qs)$ such that $0 \leqslant s < 1$, is the rectangle defined by

$$\mathbf{R}_{p,q} = \left\{ \mathbf{x} \in \mathbb{R}^2 \mid \mathbf{x} = s(p,q) + t(-q,p), 0 \leqslant s < 1, -\frac{p+q}{p^2+q^2} \leqslant t \leqslant \frac{p+q}{p^2+q^2} \right\}, \tag{26}$$

as depicted in Fig. 4. Let $\mathbb{I}_{p,q} \subset \mathbb{Z}^2$ be the set of grid points $\mathbf{z} \in \mathbb{Z}^2$ contained within this rectangle, and let $\mathbb{I}_{p,q}^{\infty} \subset \mathbb{Z}^2$ be the set of grid points $\mathbf{z} \in \mathbb{Z}^2$ in such a rectangle for which $-\infty < t < \infty$.

We have the following lemma:

**Lemma 1.** *There exist a pair of grid points* $\mathbf{z}_k^+,\ \mathbf{z}_k^- \in \mathbb{Z}^2$ *such that for any given* $k \in \mathbb{Z}^+$,

$$dist(\mathbf{z}_k^+, \Gamma_{p,q}) = dist(\mathbf{z}_k^-, \Gamma_{p,q}) = \frac{k}{\sqrt{p^2+q^2}}, \tag{27}$$

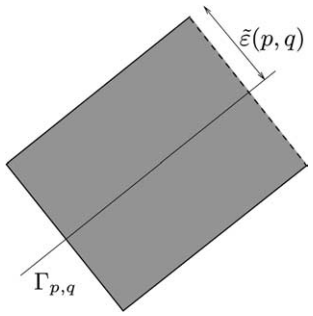


Fig. 4. The summation is done in the shaded region, the rectangle $\mathbf{R}_{p,q}$ as defined in Eq. (26), whose sides are $\sqrt{p^2+q^2}$ and $2\tilde{\varepsilon}(p,q)$.

*where dist($\mathbf{z}$, $\Gamma_{p,q}$) is the smallest Euclidean distance between $\mathbf{z}$ and any point on $\Gamma_{p,q}$. Furthermore, there are exactly two such grid points in $\mathbb{I}^{\infty}_{p,q}$ for each given $k$, and they are on different sides of $\Gamma_{p,q}$.*

**Proof.** Let $\mathbf{z} = (i,j) \in \mathbb{Z}^2$. The vector from $\Gamma_{p,q}$ to $\mathbf{z}$ orthogonal to $\Gamma_{p,q}$, can be computed by subtracting off the projection of $\mathbf{z}$ onto $\Gamma_{p,q}$ from $\mathbf{z}$. The length of this vector, which is the distance from $\mathbf{z}$ to $\Gamma_{p,q}$, is $\mathrm{dist}(\mathbf{z},\Gamma_{p,q}) = |-iq+jp|/\sqrt{p^2+q^2}$. Hence, we first need to show that there exist integers $i$, $j$ so that $|-iq+jp| = k$ for any positive integer $k$.

This is equivalent to showing the existence of integer pairs $\bar{i},\bar{j}$ satisfying

$$\bar{i}q + \bar{j}p = 1, \tag{28}$$

since we can simply multiply $\bar{i}$ and $\bar{j}$ by $-k$ and $k$, respectively, to define $i$ and $j$ and get one desired grid point with distance $k/\sqrt{p^2+q^2}$.

For any given two integers $(p, q)$, the existence of integer pair $(\bar{i},\bar{j})$ satisfying Eq. (28) is equivalent to $p$ and $q$ being relative primes [5]. Hence, our hypothesis on $p$, $q$ being relative prime guarantees the existence of $\mathbf{z}_k = (i, j)$ for any integer $k$ with $\mathrm{dist}(\mathbf{z}_k,\Gamma_{p,q}) = k/\sqrt{p^2+q^2}$.

If $(i,j) \notin \mathbb{I}^{\infty}_{p,q}$, then one of the following points have the same distance to $\Gamma_{p,q}$ : $(i+sp, j+sq) \in \mathbb{I}^{\infty}_{p,q}$ for some $s \in \mathbb{Z}$. To see this, let $i + sp = m$ and $j + sq = n$, where $i$, $j$, $m$, $n$ are some integers. So $s = (m-i)/p = (n-j)/q$ and $(m-i)q = (n-j)p$. Since $p$ and $q$ are relative primes, $q$ must be a factor of $n-j$, implying that $s = (n-j)/q$ is an integer. That there can be only one such point in $\mathbb{I}^{\infty}_{p,q}$ follows from the definition in Eq. (26). A second point on the other side of $\Gamma_{p,q}$ is given by $(p-i, q-j)$. A similar argument as above applies to this point. This proves that there are only two points $\mathbf{z}^{+}_k$ and $\mathbf{z}^{-}_k$ satisfying Eq. (27) in $\mathbb{I}^{\infty}_{p,q}$, and that they are on different sides of $\Gamma_{p,q}$. □

In addition to the points above, $\mathbf{z} = (0,0) \in \mathbb{I}_{p,q}$ and $\mathrm{dist}(\mathbf{z}, \Gamma_{p,q}) = 0$. Let us now show the following theorem.

**Theorem 3.** *The Riemann sum of $\delta^{L}_{\tilde{\varepsilon}(p,q)}(d(\Gamma_{p,q},\mathbf{x}))$ in $\mathbb{I}_{p,q}$ with*

$$\varepsilon = \tilde{\varepsilon}(p,q) = \frac{p+q}{\sqrt{p^2+q^2}} \tag{29}$$

*yields the exact length of $\Gamma_{p,q}$ within $\mathbf{R}_{p,q}$ as defined in Eq. (26), which is $\sqrt{p^2+q^2}$. Furthermore, the result is invariant under any translation of $\Gamma_{p,q} + \zeta$ for $\zeta \in [0,1)\times[0,1)$, and the Riemann sum over $\mathbb{I}_{p,q} + \zeta$.*

**Proof.** The length of $\Gamma_{p,q}$ in $\mathbb{I}_{p,q}$ is $\sqrt{p^2+q^2}$. By direct calculation, using the definition of the linear hat function, we have (with $d_k = k/\sqrt{p^2+q^2}$)

$$S = \sum_{\mathbf{j}\in\mathbb{I}_{p,q}} \delta_\varepsilon^L(d(\Gamma,\mathbf{x}_\mathbf{j})) = \frac{1}{\varepsilon} + \frac{2}{\varepsilon}\sum_{k=1}^{p+q}\left(1-\frac{d_k}{\varepsilon}\right) = \frac{1+2(p+q)}{\varepsilon} - \frac{1}{\varepsilon^2}\frac{(p+q)(p+q+1)}{\sqrt{p^2+q^2}} = \sqrt{p^2+q^2},$$

where we have used $\varepsilon = \tilde{\varepsilon}(p,q) = (p+q)/\sqrt{p^2+q^2}$. Notice that the sum over $\mathbb{T}_{p,q}$ is reduced to sum over $1 \leqslant k \leqslant p+q$ since $\delta_\varepsilon^L(d_k) = 0$ for $d_k = k/\sqrt{p^2+q^2} \geqslant (p+q)/\sqrt{p^2+q^2}$,

We now show that this result is invariant under translation. The translation $\zeta \in [0,1)\times[0,1)$ is equivalent to a displacement of $\Gamma_{p,q}$ in the normal direction with distance $\eta$ and $0 < \eta < 1/\sqrt{p^2+q^2}$. By direct summation, we have

$$S = \sum_{k=0}^{p+q}\frac{1}{\varepsilon}\left(1-\frac{1}{\varepsilon}\frac{|k-\eta|}{\sqrt{p^2+q^2}}\right) + \sum_{k=1}^{p+q-1}\frac{1}{\varepsilon}\left(1-\frac{1}{\varepsilon}\frac{k+\eta}{\sqrt{p^2+q^2}}\right).$$

Summing up the $1/\varepsilon$ terms, evaluating the terms for $k = 0$ and $k = p + q$, and combining the two sums into one (noting that the $\eta$ terms cancel out), we get

$$S = \frac{2(p+q)}{\varepsilon} - \frac{1}{\varepsilon^2}\left(\frac{\eta}{\sqrt{p^2+q^2}} + \frac{p+q-\eta}{\sqrt{p^2+q^2}}\right) - \frac{2}{\varepsilon^2}\sum_{k=1}^{p+q-1}\frac{k}{\sqrt{p^2+q^2}} = \frac{2(p+q)}{\varepsilon} - \frac{1}{\varepsilon^2}\frac{(p+q)^2}{\sqrt{p^2+q^2}}.$$

Using $\varepsilon = (p+q)/\sqrt{p^2+q^2}$, we have $S = \sqrt{p^2+q^2}$. For $\eta \geqslant 1/\sqrt{p^2+q^2}$, we can always write $\eta = (k'+\eta')/\sqrt{p^2+q^2}$, where $k' \in \mathbb{N}$, and $0 \leqslant \eta' < 1/\sqrt{p^2+q^2}$. □

For an arbitrarily long line segment with slope $q/p$, the Riemann sum can be grouped into a fixed number of sums identical to $S$ in the proof above and a finite number of terms at the end points. These finite number of terms result in an $O(h)$ error as was shown in Proof of Theorem 2.

The scaling can be extended to computing surface area in three dimensions. Define

$$\mathbf{R}_{p,q,r} = \Big\{\mathbf{x}\in\mathbb{R}^3 \mid \mathbf{x} = u(p,0,r) + v(0,q,r) + w(p,q,r), 0 \leqslant u < 1, 0 \leqslant v < 1, \\ -\frac{p+q+r}{p^2+q^2+r^2} \leqslant w \leqslant \frac{p+q+r}{p^2+q^2+r^2}\Big\} \tag{30}$$

and correspondingly let $\mathbb{I}_{p,q,r} \subset \mathbb{Z}^3$ be the set of grid points $\mathbf{z} \in \mathbb{Z}^3$ contained within this rectangle. The following theorem can then be shown by direct computation, analogous to the proof above,

**Theorem 4.** *Let $p$, $q$ and $r$ be three positive integers that are relatively prime to each other. Let $\Gamma_{p,q,q}$ be a plane passing through the origin and orthogonal to $(p, q, r)$. Then the Riemann sum of $\delta_\varepsilon^L(d(\Gamma,\mathbf{x}))$ in $\mathbb{I}_{p,q,r}$ with*

$$\varepsilon = \frac{p+q+r}{\sqrt{p^2+q^2+r^2}} \tag{31}$$

*yields the exact surface area of the the plane $\Gamma_{p,q,r}: rz = px + qy$ confined in $\mathbb{I}_{p,q,r}$. Furthermore, this result is invariant under any translation of $\Gamma_{p,q,r} + \zeta$, $\zeta \in [0, 1)^3$.*

Motivated by the above results, we propose an approximate delta function for a general $\Gamma$,

$$\delta^L_{\varepsilon(\nabla d,\varepsilon_0)}(d(\Gamma,\mathbf{x})), \tag{32}$$

as based on the one-dimensional linear hat function $\delta_\varepsilon^L$, but with $\varepsilon$ scaled according to how $\Gamma$ lies in the given Cartesian grid.

Hence, given the distance function to $\Gamma$, $d(\Gamma, \mathbf{x})$, we let $p = |\frac{\partial}{\partial x}d(\Gamma,\mathbf{x})|, q = |\frac{\partial}{\partial y}d(\Gamma,\mathbf{x})|$, and define $\varepsilon$ according to Eq. (29). Additionally, in three dimensions, we define $r = |\frac{\partial}{\partial z}d_\Gamma|$, and set $\varepsilon$ according to

Eq. (31). We remark that the denominators $\sqrt{p^2+q^2}$ and $\sqrt{p^2+q^2+r^2}$ are equal to $|\nabla d|$ in two and three dimensions, respectively. Furthermore, we note that $p+q$ and $p+q+r$, are the pointwise 1-norms of $\nabla d(\mathbf{x})$ in two and three dimensions, respectively. Denote the 1 norm of a vector $\mathbf{v}$ by $|\mathbf{v}|_1$, and using this, define

$$\varepsilon(\mathbf{v}, \varepsilon 0) = \frac{|\mathbf{v}|_1}{|\mathbf{v}|}\varepsilon_0. \tag{33}$$

With $\mathbf{v} = \nabla d$, the regularization parameter in Eq. (32) simplifies to $\varepsilon(\nabla d, \varepsilon_0) = |\nabla d|_1 \varepsilon_0$ since $|\nabla d| = 1$ for the signed distance function.

## 4. Numerical results

### 4.1. Quadrature

In this section, we compute the discretization error $E$, as defined in Eq. (6), for a few different choices of curves $\Gamma \in \mathbb{R}^2$, and functions $f(\mathbf{x})$. We test both new approaches as described in the previous sections. We define $\tilde{\delta}_\varepsilon(\Gamma, \mathbf{x})$ using the approximate product formula, as in Eq. (18), and $\delta^L_{\varepsilon(\nabla d, \varepsilon_0)}(d(\Gamma, \mathbf{x}))$ as in (32), with the variable regularization parameter $\varepsilon(\nabla d, \varepsilon_0)$ as defined in Eq. (33).

First, let $\Gamma$ be a circle with radius $r = 0.35\sqrt{2}$, centered in $(x_0, y_0)$. The relative integration error for this $\Gamma$ has been computed with both $f \equiv 1$ and $f = \mathrm{e}^r - \sqrt{(x-x_0)^2 + (y-y_0)^2}$, see the two left most plots in Fig. 5. In the right most plot in the same figure, the relative integration errors for the capsule shaped $\Gamma$ as in Fig. 1 (with $a = 0.12\sqrt{2}$, $L = 2$), and $f \equiv 1$ have been plotted. To compute the relative integration errors, the numerical results are averaged over 64 small irregular shifts in the grid in each of these cases, and the error is normalized using the exact value of the integral. This procedure reveals the convergence of the mean error which is less sensitive to the error constant that fluctuates according to the placement of $\Gamma$ in a grid.

In Fig. 5, we note that the approximate product rule yields the best results. The average error shows a second-order convergence. For the variable $\varepsilon$ approach, the errors are larger, and the convergence rates are fluctuating more. On average, we have better than first order, but not second-order convergence.

Let us now define $f(\mathbf{x}) = \nabla \tilde{f} \cdot \mathbf{n}_\Gamma$, where $\mathbf{n}_\Gamma$ is the normal vector to $\Gamma$, pointing into the region where $d(\Gamma, \mathbf{x}) > 0$. We have that $\mathbf{n}_\Gamma = \nabla d(\Gamma, \mathbf{x})$, and so we write

$$\int_\Gamma f(\mathbf{X}(s))\,\mathrm{d}s = \int_\Gamma \nabla \tilde{f} \cdot n_\Gamma\,\mathrm{d}s = \int_{\mathbb{R}^2} \nabla \tilde{f} \cdot \nabla d(\Gamma, \mathbf{x}) \delta(\Gamma, \mathbf{x})\,\mathrm{d}\mathbf{x}. \tag{34}$$

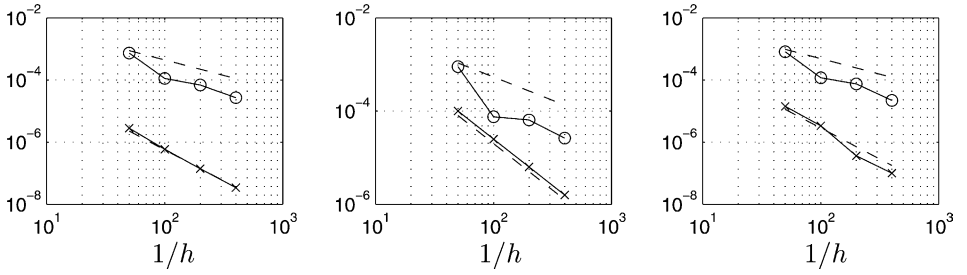


Fig. 5. The relative error in the integration for, from left to right: $\Gamma$ circle, $f \equiv 1$; $\Gamma$ circle, $f = \mathrm{e}^{r - \sqrt{(x-x_0)^2+(y-y_0)^2}}$; $\Gamma$ capsule, $f \equiv 1$. Delta approximation $\delta^L_{\epsilon(\nabla d, h)}$ (○), (variable $\varepsilon$), and $\tilde{\delta}^L_h$ (×) (approximate product rule). Error averaged over 64 shifts in the grid. The dashed lines in the plots are proportional to $h$ and $h^2$.

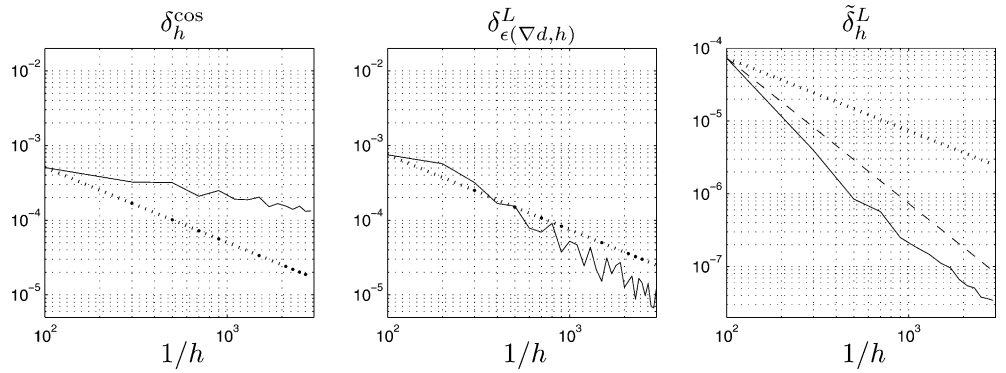


Fig. 6. The discretization error $E$ as defined in Eq. (6) for different delta function approximations for the line integral in Eq. (34). From left to right: $\delta_h^{\cos}(d(\Gamma,\mathbf{x}))$ (constant $\varepsilon = h$), $\delta^L_{\epsilon(\nabla d,h)}(d(\Gamma,\mathbf{x}))$ (variable $\varepsilon$), and $\tilde{\delta}^L_h$ (approximate product rule). The solid lines represent the computed error. The dotted and dashed lines are proportional to $h$ and $h^2$, respectively.

This integral evaluates to zero for $f \in C^1(\mathbb{R}^2)$. It is therefore a good test case, since the exact result is known for any such choice of $\tilde{f}$, independent on the choice of $\Gamma$.

In Fig. 6, we show the integration errors for this case, with $\Gamma$ the capsule shaped curve as in Fig. 1 (with $a = 0.1\sqrt{2}$ and $L = 1.4$), and with $\tilde{f}(\mathbf{x}) = \tilde{f}(x,y) = \cos(x)\sin(y)$. The errors have been averaged over 25 small irregular shifts in the grid.

The inconsistent formulation $\delta_h^{\cos}(d(\Gamma,\mathbf{x}))$ as based on the cosine formula in Eq. (13), with a constant $\varepsilon = h$, is included for comparison, since this has been a frequently used approximation in connection to level set methods. The capsule shape is in this case not as elongated as for the results presented in Fig. 2 in Section 2 for the linear hat functions, where the error did not decay at all. Here, the cancellation of errors in the circle regions does yield some decay as we refine. However, the convergence rate is clearly lower than first order.

In agreement with Fig. 5, the other results show that the delta approximation $\delta^L_{\epsilon(\nabla d,h)}$ with a variable regularization parameter $\varepsilon$ yields a first order convergence, whereas the delta approximation based on the approximate product rule, $\tilde{\delta}^L_h$, yields an error of significantly smaller magnitude, converging to second order.

Hence, simply using a variable regularization parameter $\varepsilon(\nabla d, \varepsilon_0)$, when defining $\delta^L_\varepsilon(d(\Gamma,\mathbf{x}))$ turns an inconsistent approximation into one with a first order convergence in grid size. This is indicated in numerical tests, but not proven for general $\Gamma$. However, if smaller errors are desirable, it is worth implementing the approximate product rule to define $\tilde{\delta}^L_h$, which yields a second-order approximation. This approximation is again based solely on the distance function $d(\Gamma, \mathbf{x})$ and its gradient, as described in Section 3.1.

### 4.2. Applications to a class of partial differential equations

In the previous sections, we have discussed the regularization of singular integrands in numerical quadrature. The results from this analysis are applicable also for source term regularization in the numerical solution of differential equations when the location of the source term singularity is given by a level set formulation.

The solution of a differential equation,

$$Lu = s(\mathbf{x}), \quad \mathbf{x} \in \Omega \subset \mathbb{R}^d, \qquad Bu = r(\mathbf{x}), \quad \mathbf{x} \in \partial\Omega, \tag{35}$$

can be given as an integral of the fundamental solution $G(\mathbf{x}, \mathbf{y})$ multiplying the source term $s(\mathbf{x})$,

$$u(\mathbf{x}) = \int_\Omega G(\mathbf{x},\mathbf{y}) s(\mathbf{y})\, d\mathbf{y} + R(\mathbf{x}), \tag{36}$$

where $R(\mathbf{x})$ represents the contribution from the boundary conditions. The solution of a corresponding numerical approximation can be written on the form

$$u_{\mathbf{j}} = \left(\prod_{k=1}^{d} h_k\right) \sum_{\mathbf{m}\in\Omega_h} G_{\mathbf{jm}} s_{\mathbf{m}} + R_{\mathbf{j}}, \tag{37}$$

where $G_{\mathbf{jm}}$ is the discrete fundamental solution and $\Omega_h$ is the index set for the grid points inside $\Omega$. $G_{\mathbf{jm}}$ will be determined by the specific numerical approximation that is used.

Now, let $s(\mathbf{y}) = \delta(\Gamma, g, \mathbf{y})$ in Eq. (36). We will consider the solution for $\mathbf{x}$ values away from the discontinuity and thus assume that $|\mathbf{x} - \mathbf{y}| \geqslant C > \varepsilon$ for all $\mathbf{y} \in \Gamma$, and furthermore that $\delta(\Gamma, g, \mathbf{y})$ has compact support away from the boundaries of $\Omega$.

We use a regularized delta function for the discrete approximation, and define $s_{\mathbf{m}} = \delta_\varepsilon(\Gamma, g, \mathbf{x}_{\mathbf{m}})$ in Eq. (37). Considering homogeneous boundary conditions, we have that $u(\mathbf{x})$ is given by Eq. (36) with $R(\mathbf{x}) = 0$ and $u_{\mathbf{j}}$ by Eq. (37) with $R_{\mathbf{j}} = 0$ and where the summation over $\mathbf{m}$ can be replaced by $\mathbf{m} \in Z^d$. We can then write the pointwise difference between the exact solution and the numerical solution as

$$|u(\mathbf{x}_{\mathbf{j}}) - u_{\mathbf{j}}| = \left| \int_\Omega G(\mathbf{x}_{\mathbf{j}}, \mathbf{y}) \delta(\Gamma, g, \mathbf{y})\, \mathrm{d}\mathbf{y} - \left(\prod_{k=1}^{d} h_k\right) \sum_{\mathbf{m}\in Z^d} G_{\mathbf{jm}} \delta_\varepsilon(\Gamma, g, \mathbf{x}_{\mathbf{m}}) \right|$$

and so

$$\begin{aligned} |u(\mathbf{x}_{\mathbf{j}}) - u_{\mathbf{j}}| &\leqslant \left| \int_\Omega G(\mathbf{x}_{\mathbf{j}}, \mathbf{y}) \delta(\Gamma, g, \mathbf{y})\, \mathrm{d}\mathbf{y} - \left(\prod_{k=1}^{d} h_k\right) \sum\nolimits_{\mathbf{m}\in Z^d} G(\mathbf{x}_{\mathbf{j}}, \mathbf{x}_{\mathbf{m}}) \delta_\varepsilon(\Gamma, g, \mathbf{x}_{\mathbf{m}}) \right| \\ &\quad + \left| \left(\prod_{k=1}^{d} h_k\right) \sum\nolimits_{\mathbf{m}\in Z^d} \left[G(\mathbf{x}_{\mathbf{j}}, \mathbf{x}_{\mathbf{m}}) - G_{\mathbf{jm}}\right] \delta_\varepsilon(\Gamma, g, \mathbf{x}_{\mathbf{m}}) \right| \\ &= \mathrm{I} + \mathrm{II}. \end{aligned} \tag{38}$$

The first part (I) of the error is the type of quadrature error discussed in the previous section, where the function multiplying the delta function is the Green's function for the continuous problem. We here assume that $\delta_\varepsilon(\Gamma, g, \mathbf{x}_{\mathbf{m}})$ is such that this error is $\mathrm{O}(h^q)$. This argument requires that *the Green's function* $G(\mathbf{x}, \mathbf{y})$ *be regular away from* $\mathbf{x} = \mathbf{y}$, which is true for a large class of problems.

Furthermore, if the numerical approximation of the partial differential equation is of order $p$ with

$$|G_{\mathbf{jm}} - G(\mathbf{x}_{\mathbf{j}}, \mathbf{x}_{\mathbf{m}})| \leqslant C_1 h^p$$

away from $\mathbf{x}_{\mathbf{j}} = \mathbf{x}_{\mathbf{m}}$, then part (II) of the error is of order $p$ and the total error is

$$|u_{\mathbf{j}} - u(\mathbf{x}_{\mathbf{j}})| \leqslant C_2 h^{\min(p,q)}, \tag{39}$$

when $|\mathbf{x}_{\mathbf{j}} - \mathbf{x}| \geqslant C > \varepsilon$ for all $\mathbf{x} \in \Gamma$.

Hence, the numerical error is a combination of the discretization error made for the differential equation and the quadrature error for the regularized delta function.

In more than one spatial dimension, with $\delta_\varepsilon(\Gamma, \mathbf{x}) = \delta_\varepsilon(d(\Gamma, \mathbf{x}))$, there are cases where the quadrature error is O(1), as discussed in the previous section and in [13]. Because of the estimate above, the poor accuracy for the quadrature is expected to carry over to the solutions of differential equations, which was also shown in [13].

With the improved $\delta_\varepsilon$ approximations for several dimensions introduced in this paper, the quadrature errors are smaller, and hence, we expect also the results for the solutions of differential equations to improve.

Let us consider the Poisson equation in $\mathbb{R}^2$,

$$Lu = -\Delta u = \delta(\Gamma, \mathbf{x}), \quad \mathbf{x} \in \Omega \subset \mathbb{R}^2,$$

$$u(\mathbf{x}) = v(\mathbf{x}), \quad \mathbf{x} \in \partial\Omega,$$

where $\Omega = \{\mathbf{x} = (x,y);\ |x| \leqslant 1,\ |y| \leqslant 1\}$. With $\Gamma$ a circle, $\Gamma = \{\mathbf{x}, |\mathbf{x} - \bar{\mathbf{x}}| = 1/2\}$, and $v(\mathbf{x}) = 1 - \log(2|\mathbf{x} - \bar{\mathbf{x}}|)/2$, this equation has the following solution:

$$u(\mathbf{x}) = \begin{cases} 1, & |\mathbf{x} - \bar{\mathbf{x}}| \leqslant 1/2, \\ 1 - \log(2|\mathbf{x} - \bar{\mathbf{x}}|)/2, & |\mathbf{x} - \bar{\mathbf{x}}| > 1/2. \end{cases} \tag{40}$$

This solution has been plotted in Fig. 7.

We introduce a $N \times N$ uniform grid, with step size $h = 2/N$ in both $x$ and $y$. To discretize the second derivatives, we use the standard centered second-order stencil.

The two new techniques for regularizing the delta function introduced in this paper have been tested. The first one is to define $\tilde{\delta}_\varepsilon(\Gamma, \mathbf{x})$ by the approximate product rule as defined in Eq. (18). Secondly, we define $\delta^L_{\varepsilon(\nabla d, \varepsilon_0)}(d(\Gamma, \mathbf{x}))$, with the variable regularization parameter $\varepsilon(\nabla d, \varepsilon_0)$ as defined in Eq. (33). In Fig. 8, the results are plotted for the case when the circle is centered in $\bar{\mathbf{x}} = (0,0)$. To measure the error away from $\Gamma$, we introduce the sub-domain

$$\tilde{\Omega} = \{\mathbf{x} : \mathbf{x} \in \Omega, |d(\Gamma, \mathbf{x})| > \beta\}.$$

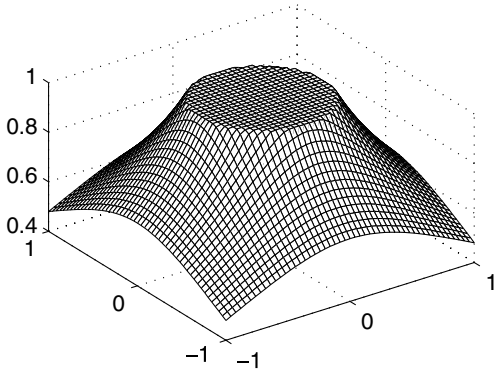


Fig. 7. Solution $u(\mathbf{x})$ as in Eq. (40) for $\bar{\mathbf{x}} = 0$.

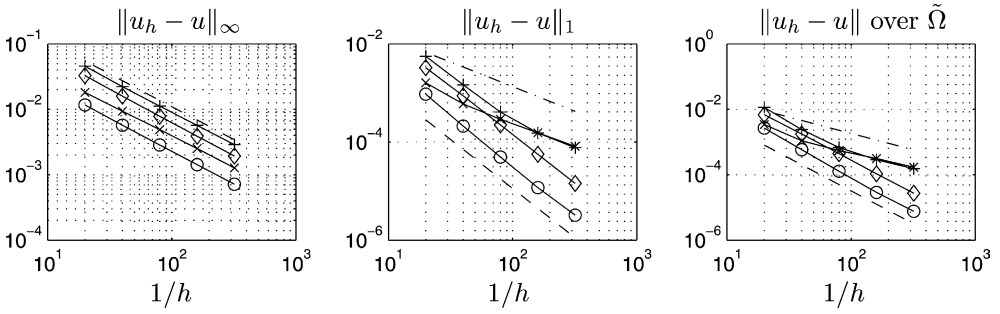


Fig. 8. The errors in different norms for: variable $\varepsilon$, with $\varepsilon_0 = h$ (×) and $\varepsilon_0 = 2h$ (+), approximate product rule, $\varepsilon = h$ (○) and $\varepsilon = 2h$ (◇). In the right most frame, the maximum norm is measured over $\tilde{\Omega}$. The dash-dotted and dashed lines in the plots are proportional to $h$ and $h^2$, respectively. $\bar{\mathbf{x}} = (0,0)$.

We pick $\beta = 0.2$, which is $2h$ in the coarsest grid, and check the convergence in the maximum norm when measured over this domain. The result is plotted in the right most frame in Fig. 8.

Clearly, we have a first-order error in maximum norm in all cases (with the maximal error close to $\Gamma$). For the approximate product rule, the L1-error is second order, as well as the maximum error when measured away from $\Gamma$.

For the variable $\varepsilon$ approach, with $\bar{\mathbf{x}} = (0, 0)$, in Fig. 8 we see that the convergence in $L1$ as well as the cut maximum norm, starts out with higher than first order, coming down to first order as we refine. This error depends on shifts of $\Gamma$ relative to the grid. For this approximation, there is a first-order component of the error, but it does not in all cases clearly dominate over the second-order term, and for some shifts, we can note a more mixed result, and a convergence rate closer to two.

For both approaches, the results are better for the more narrow discretization, with $\varepsilon_0 = h$ and $\varepsilon = h$, respectively.

For comparison, in Fig. 9, we also plot the results for $\delta_\varepsilon^L(d(\Gamma, \mathbf{x}))$ with a constant regularization parameter $\varepsilon$. For these approximations, we showed for a specific example in Section 2 that the error in the integration is O(1). As we refine, we therefore expect that the non-decaying part of the error, part I in Eq. (38) should dominate and hence that the error curves flatten out for smaller grid sizes $h$. It is clear that the new consistent techniques introduced in this paper yield much better results also in this case.

Lastly, we point out that, for the types of PDEs that are considered above, the solutions are continuous. But the proposed technique could in principle also be applied to problems whose solutions have jump discontinuities. As an example, consider

$$\begin{cases} \frac{\mathrm{d}u}{\mathrm{d}x} = \delta_\Gamma(x) = \delta(x - \tilde{x}), \quad \tilde{x} > 0, \\ u(0) = 0. \end{cases} \tag{41}$$

The exact solution is $u(x) = H(x - \tilde{x})$. Explicit Euler's method yields the exact solution away from the jump, if the zero-order moment condition is satisfied. More precisely,

$$u_{j+1} = u_j + h\delta_\varepsilon(x_j - \tilde{x}),$$

so $u_j = h\sum_j \delta_\varepsilon(x_j - \tilde{x}) = 1$ for $x_j \geqslant \tilde{x} + \varepsilon$. Our proof, however, does not cover this type of problems.

If instead, we consider

$$u_{xx} = \delta_\Gamma(x) = \delta_\varepsilon(x - \tilde{x})$$

and $x_k \leqslant \tilde{x} \leqslant x_{k+1}$, then standard central differencing for $u_{xx}$ at $x_k$ and $x_{k+1}$ would read, respectively,

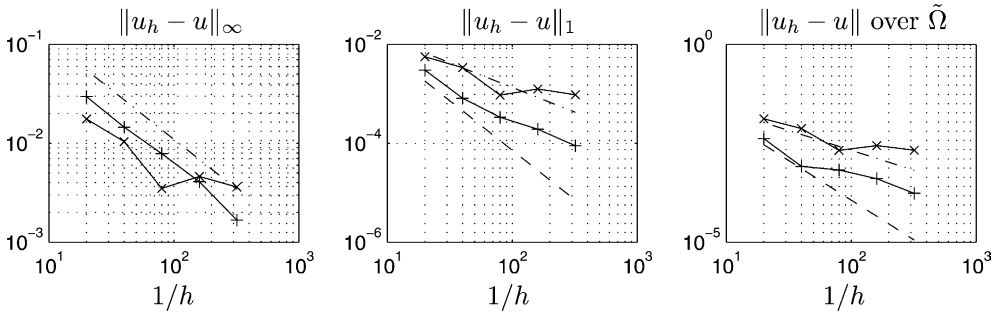


Fig. 9. The errors in different norms for $\delta_\varepsilon^L(d(\Gamma, \mathbf{x}))$ with a constant regularization parameter $\varepsilon = h$ (×), $\varepsilon = 2h$ (+). The dash-dotted and dashed lines in the plots are proportional to $h$ and $h^2$, respectively. $\bar{\mathbf{x}} = (0, 0)$.

$$\frac{u_{k+1} - 2u_k + u_{k-1}}{h^2} = \frac{1-\theta}{h}$$

and

$$\frac{u_{k+2} - 2u_{k+1} + u_k}{h^2} = \frac{\theta}{h},$$

where $\theta = \frac{\tilde{x}-x_k}{h}$ and $\delta_\varepsilon(x) = \delta_h^L(x-\tilde{x})$. We remark that this discretization is similar to what is derived in the ghost fluid method [7] for the above equation.

## 5. Extensions

### 5.1. Non-distance level set functions

The algorithms developed in Section 3 are based on the use of the signed distance function to $\Gamma$, $d(\Gamma, \mathbf{x})$, as defined in Eq. (3). Now, let $\Gamma$ be defined as the zero level set of a level set function $\phi$. If $\phi$ is not a signed distance function, we can perform reinitialization to reshape this level set function into the distance function of $\Gamma$, see [8,10] for details. However, in numerical simulations with moving boundaries, one might not wish to perform such a reinitialization very frequently due to computational cost and accumulation of numerical errors in the location of these boundaries.

If the level set function $\phi$ is not a distance function, one cannot simply replace the distance function by $\phi$ in the formulas derived in Section 3, since that can again lead to O(1) errors.

To see why this is the case, let $\phi(x)$ be the one-dimensional level set function: $\phi(x) = px$, with $p$ a positive real number. (with $p = 1$, $\phi$ is a distance function). The half-width support of $\delta_\varepsilon^L(\phi(x))$ in physical space is $\varepsilon/p = \varepsilon/|\phi_x|$. In order for even the lowest one-dimensional moment condition (i.e., the mass condition) to be fulfilled, we need this support to be $\varepsilon = mh$, where $m$ is an integer and $h$ is the grid size, which is in general not the case for $p \neq 1$. Hence, for $p \neq 1$, there will be an O(1) error. In this case, a simple remedy is to scale the argument, and define $\delta_\varepsilon(\phi/|\phi_x|)$.

So what about a more general $\phi(\mathbf{x})$ in more than one dimension? Let $\mathbf{x}_0 \in \Gamma$, i.e., such that $\phi(\mathbf{x}_0) = 0$, and consider the Taylor expansion

$$\phi(\mathbf{x}) = (\mathbf{x} - \mathbf{x}_0) \cdot \nabla\phi + R_\phi |\mathbf{x} - \mathbf{x}_0|^2,$$

with the remainder coefficient $R_\phi$ bounded. The linear approximation $\Gamma_h$ of $\Gamma$ from $\mathbf{x}$ is $(\mathbf{x} - \mathbf{x}_0) \cdot \nabla\phi - \phi(\mathbf{x}) = 0$, implying that the distance between the closest point $\mathbf{x}_0 \in \Gamma_h$ to $\mathbf{x}$ is

$$|\mathbf{x} - \mathbf{x}_0| \sim \frac{\phi(\mathbf{x})}{|\nabla\phi(\mathbf{x})|}.$$

Hence, given $\phi$, we can use $\phi/|\nabla\phi|$ near its zeros as an approximation to $d(\Gamma, \mathbf{x})$ and use $\varepsilon(\nabla\phi, \varepsilon_0)$ (with $\varepsilon$ as defined in Eq. (33)) to define the delta approximation as

$$\delta_{\varepsilon(\nabla\phi,\varepsilon_0)}\left(\frac{\phi(\mathbf{x})}{|\nabla\phi|}\right). \tag{42}$$

Using the definition of $\delta_\varepsilon$ in Eq. (11), for $|\phi|/|\nabla\phi| \leqslant \varepsilon = \varepsilon(\nabla\phi, \varepsilon_0)$ we can write

$$\delta_\varepsilon\left(\frac{\phi}{|\nabla\phi|}\right) = \frac{1}{\varepsilon}\psi\left(\frac{\phi/|\nabla\phi|}{\varepsilon}\right) = \frac{1}{\varepsilon|\nabla\phi|}\psi\left(\frac{\phi}{\varepsilon|\nabla\phi|}\right)|\nabla\phi| = \frac{1}{\tilde{\varepsilon}}\psi\left(\frac{\phi}{\tilde{\varepsilon}}\right)|\nabla\phi| = \delta_{\tilde{\varepsilon}}(\phi)|\nabla\phi|,$$

with $\tilde{\varepsilon} = \varepsilon|\nabla\phi|$. Again, $\delta_{\tilde{\varepsilon}}$ is non-zero for $\phi \leqslant \tilde{\varepsilon} = \varepsilon|\nabla\phi|$, which is the same condition as above.

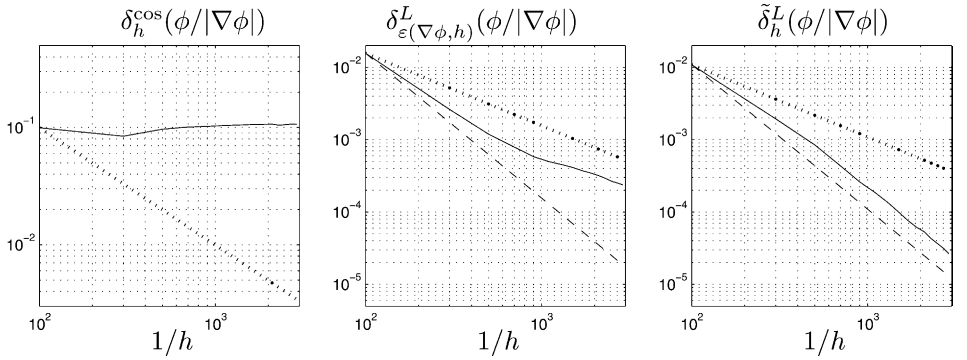


Fig. 10. The discretization error $E$ as in Fig. 6, but with delta approximations based on a non-distance level set function $\phi$, as defined in Eq. (44). From left to right: $\delta_h^{\cos}(\phi/|\nabla\phi|)$ (constant $\varepsilon$), $\delta^L_{\varepsilon(\nabla\phi,h)}(\phi/|\nabla\phi|)$ (variable $\varepsilon$), and $\tilde{\delta}^L_h(\phi/|\nabla\phi|)$ (approximate product rule). The solid lines represent the computed error. The dotted and the dashed lines are proportional to $h$ and $h^2$, respectively.

Now, we have $\tilde{\varepsilon} = \varepsilon|\nabla\phi| = \varepsilon_0|\nabla\phi|_1$, from the definition of $\varepsilon = \varepsilon(\nabla\phi/|\nabla\phi|, \varepsilon_0)$ in Eq. (33). Here, $|\nabla\phi|_1$ is the pointwise 1-norm of $\nabla\phi$. Hence, we have that

$$\delta_{\varepsilon(\nabla\phi,\varepsilon_0)}\left(\frac{\phi(\mathbf{x})}{|\nabla\phi|}\right) = \delta_{\varepsilon_0|\nabla\phi|_1}(\phi(\mathbf{x}))|\nabla\phi|. \tag{43}$$

As an approximation to the integral over $\delta(\Gamma,\mathbf{x})\, f(\mathbf{x})$, this yields

$$\int \delta_{\varepsilon(\nabla\phi,\varepsilon_0)}\left(\frac{\phi(\mathbf{x})}{|\nabla\phi|}\right) f(\mathbf{x})\, \mathrm{d}\mathbf{x} = \int \delta_{\varepsilon_0|\nabla\phi|_1}(\phi(\mathbf{x}))|\nabla\phi| f(\mathbf{x})\, \mathrm{d}\mathbf{x},$$

which can be compared to the scaling of the non-regularized $\delta$-function in Eq. (4).

If $|\nabla\phi|$ is non-constant, this approximation of the delta function is not equivalent, but rather only an approximation, to the definition using the distance function. However, if $\phi$ is smooth and $\nabla\phi \neq 0$, with a small $\varepsilon_0$ such as $\varepsilon_0 = h$, it is a reasonable approximation within the region of support of the delta function.

This discussion was carried out for the variable $\varepsilon$ regularization. The same scalings can be made for the approximate product formula.

Let us now repeat the numerical experiment, for which the results were displayed in Fig. 6, but in difference to that case, with the delta approximations based on a non-distance function. Let $d(\Gamma, \mathbf{x}) = d(\Gamma, x, y)$ be the distance function to $\Gamma$, where $\Gamma$ is the capsule shaped curve (Fig. 1) with $a = 0.1\sqrt{2}$ and $L = 1.4$. Define

$$\phi(x,y) = d(\Gamma,x,y)(\sin(4\pi x) + 2)(\cos(2\pi y) + 1.6). \tag{44}$$

This is a function with the same zero level sets as $d(\Gamma, \mathbf{x})$ (i.e., $\Gamma$), but that is no longer a distance function.

We now use $\phi$ in the delta approximations, and define $\delta_h^{\cos}(\phi/|\nabla\phi|)$, $\delta^L_{\varepsilon(\nabla\phi,h)}(\phi/|\nabla\phi|)$ (the variable $\varepsilon$ approach) and $\tilde{\delta}^L_h(\phi/|\nabla\phi|)$ (the approximate product rule). We compute the discretization errors as defined in Eq. (6) for the line integral in Eq. (34), with $\tilde{f}(\mathbf{x}) = \tilde{f}(x,y) = \cos(x)\sin(y)$. We average the errors over 25 small irregular shifts of $\Gamma$ in the grid.

The results presented in Fig. 10, should be compared to those shown in Fig. 6. The only difference is that the delta approximations is based on the level set function $\phi$ as defined in Eq. (44) instead of on a distance function. Comparing these two figures, we can see that the magnitudes of the errors are much larger in this case, where we use a level set function that is not a distance function. The non-convergence of the constant $\varepsilon$ cosine approximation is apparent in this case. Concerning the convergence of the two other approaches, the

variable $\varepsilon$ approximation shows a convergence that is at least first order, and even the second-order convergence of the approximate product rule is retained.

### 5.2. Regularization of characteristic functions

Singularities of lower order than that of the delta function are also common in computations of integrals and differential equations. One such example closely related to the delta function is the characteristic function of a set

$$\chi(\Omega, \mathbf{x}) = \begin{cases} 1, & \mathbf{x} \in \Omega \subset \mathbb{R}^d, \\ 0, & \mathbf{x} \notin \Omega. \end{cases}$$

Regularization of the characteristic function for a domain is used to represent piecewise smooth functions, [8,10,15,16], and to define volume integrals of a closed domain $\Omega$. In the context of level set methods, $\chi(\Omega, \mathbf{x})$ can conveniently be expressed as $H(d(\Gamma, \mathbf{x}))$, where $\{\mathbf{x} \in \mathbb{R}^d : d(\Gamma, \mathbf{x}) \geqslant 0\} = \Omega$, and $H(x)$ is the so-called Heaviside function. Thus, we can write

$$\int_\Omega f(\mathbf{x})\, \mathrm{d}\mathbf{x} = \int_{\mathbb{R}^d} H(d(\Gamma, \mathbf{x})) f(\mathbf{x})\, \mathrm{d}\mathbf{x}. \tag{45}$$

One can develop discretely regularized characteristic functions based on the principles of Section 3.2 which produce high order of numerical accuracy. Define

$$\chi_\varepsilon(\Omega, \mathbf{x}) = \int_\Omega \prod_{k=1}^{d} \delta_{\varepsilon_k}(x^{(k)} - \xi^{(k)})\, \mathrm{d}\boldsymbol{\xi},$$

where $\delta_{\varepsilon_k}$ is defined in Eq. (11) and we assume that $\Omega$ is bounded in $\mathbb{R}^d$. Tornberg and Engquist showed in [13] that this regularization yields a discretization error bounded by $Ch^q$, if the one-dimensional delta function is of moment order $q$.

This approach is however computationally complex since the construction of $\chi_\varepsilon$ requires quadrature over a general domain $\Omega$. It is practically much more convenient to base the multidimensional regularization on a regularized one-dimensional Heaviside function by $H_\varepsilon(d(\Gamma, \mathbf{x}))$, with $\varepsilon = \varepsilon(\nabla d, h)$ as defined in Eq. (33). The one-dimensional regularized Heaviside function is given by

$$H_\varepsilon(x) = \begin{cases} 0, & x \leqslant -\varepsilon, \\ \frac{1}{2}\left(1 + \frac{x}{\varepsilon}\right), & -\varepsilon < x \leqslant \varepsilon, \\ 1, & x > \varepsilon. \end{cases} \tag{46}$$

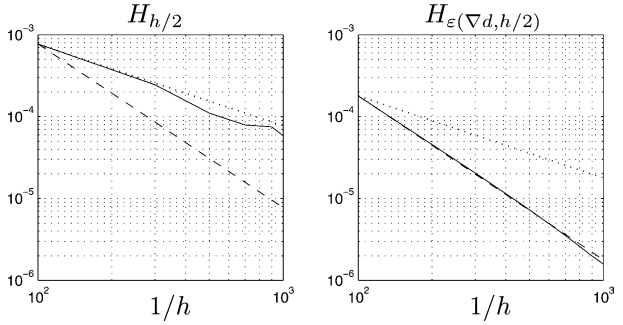


Fig. 11. Discretization error $E_\Omega$. The plot on the left shows the error from using $H_{h/2}(d(\Gamma, \mathbf{x}))$ and the plot on the right using $H_{\varepsilon(\nabla d,\, h/2)}(d(\Gamma, \mathbf{x}))$ (solid lines). The dotted and dashed lines are proportional to $h$ and $h^2$, respectively.

Below, we will show numerically, that this approach yields a second-order accurate approximation of the integral in Eq. (45).

Again let $\Gamma$ be the capsule shaped curve (Fig. 1) with $a = 0.1\sqrt{2}$ and $L = 1.4$, and let $\Omega$ be the region enclosed by $\Gamma$. We compute the integral in Eq. (45) numerically for $f \equiv 1$, with the regularized characteristic function, and define the discretization error $E_\Omega$ as

$$E_\Omega = \left| h^2 \sum_{\mathbf{j} \in Z^2} H_\varepsilon(d(\Gamma, \mathbf{x_j})) - \int_\Omega d\mathbf{x} \right|. \tag{47}$$

In Fig. 11, this discretization error (averaged over shifts in the grid) is plotted both using a variable $\varepsilon = \varepsilon(\nabla d, h/2)$, and with a constant $\varepsilon_0 = h/2$, to compare. While the errors for the regularization with constant $\varepsilon$ show only a first-order convergence, the convergence increases to second order as we introduce the variable regularization, resulting in errors of much smaller magnitude.

### 5.3. Higher dimensions

The new algorithms presented in Section 3 can both be extended to three dimensions. The variable $\varepsilon$ approach easily takes a distance function $d(\Gamma, \mathbf{x})$, $\Gamma, \mathbf{x} \in \mathbb{R}^3$ as its argument, with $\varepsilon$ still defined by Eq. (33). In case of the approximate product rule, one then needs to integrate not over piecewise tangent lines to $\Gamma$, intersecting the support of the product of one-dimensional $\delta$ approximations, but rather over tangent planes. This can still be accomplished using only the distance function and its gradient.

Let us present one numerical example for the variable $\varepsilon$ approach. Define $f(\mathbf{x}) = \operatorname{curl} \mathbf{F} \cdot \mathbf{n}_\Gamma$, where $\mathbf{n}_\Gamma$ is principal the normal vector to $\Gamma$, pointing into the region where $d(\Gamma,\mathbf{x}) > 0$. We have that $\mathbf{n}_\Gamma = \nabla d(\Gamma, \mathbf{x})$, and so we write

$$\int_\Gamma \operatorname{curl} \mathbf{F} \cdot \mathbf{n}_\Gamma \, dS = \int_{\mathbb{R}^3} \operatorname{curl} F \cdot \nabla d(\Gamma, \mathbf{x}) \delta(\Gamma, \mathbf{x}) \, d\mathbf{x}. \tag{48}$$

By Stokes theorem, if $F$ is a $C^1$ vector field in $\mathbb{R}^3$, the integral evaluates to be zero. In this example, we will use $\mathbf{F}(x, y, z) = (y^2, z^2, x^2)$.

We let $\Gamma$ be the union of two half spheres and a cylinder connecting them (see Fig. 12). The center axis of the cylinder is parallel to the vector (1, 1, 1) and has length $L = 1.5$. The shared radius of the cylinder and the spheres is $r = 0.2$. The centers of the two spheres are $\mathbf{x}_1 = (-0.7, -0.7, -0.7)$ and $\mathbf{x}_2 = (0.8, 0.8, 0.8)/\sqrt{3}$.

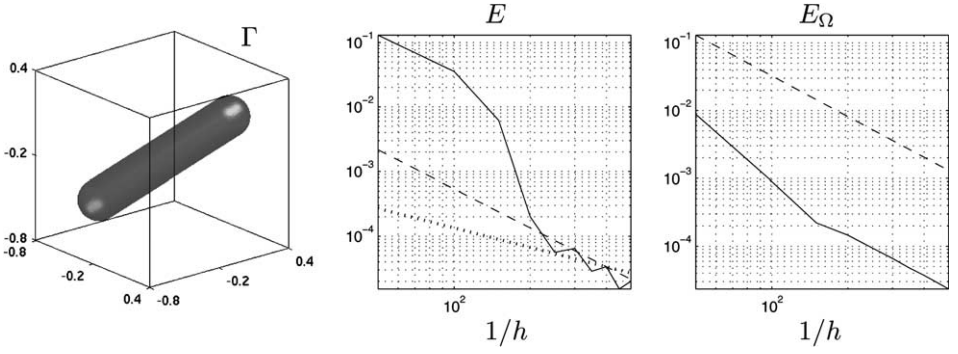


Fig. 12. From left to right, the plots show $\Gamma$, the discretization error $E$ for $\delta_\varepsilon$ and $E_\Omega$ for $H_\varepsilon$, both with $\varepsilon = \varepsilon(\nabla d, h)$. The dotted and dashed lines are proportional to $h$ and $h^2$, respectively.

We numerically compute the integral to the right in Eq. (48) with $\delta_{\varepsilon(\nabla d,\ h)}(d(\Gamma, \mathbf{x}))$, and compute the discretization error $E$ according to Eq. (6). The discretization errors are averaged over 100 small irregular shifts of the position of $\Gamma$, and the result is shown in the left plot of Fig. 12. In the right plot of the same figure, we show the error $E_\Omega$ in computing the volume of $\Omega$, the region enclosed by $\Gamma$. This is the three-dimensional version of $E_\Omega$ as defined in Eq. (47), with $H_{\varepsilon(\nabla d,\ h)}(d(\Gamma, \mathbf{x}))$, with $H_\varepsilon(x)$ as defined in Eq. (46).

In some applications, one needs to compute delta functions concentrating on a higher codimensional manifold $\Gamma$, such as curves in three dimensions, or, in general, $d$ dimensional manifolds in $\mathbb{R}^{2d}$. Typically in the corresponding level set methods, e.g. [4], the manifold in question is implicitly defined as the zeros of a system of level set functions, and additional quantities defined on the manifolds, extended to the whole space, are also tracked. The delta function is then used to extract these quantities from $\Gamma$. Assume that $\Gamma$ is a curve in three dimensions, and $\Gamma = \{\mathbf{x} \in \mathbb{R}^3 : \phi_1(\mathbf{x}) = 0, \phi_2(\mathbf{x}) = 0\}$. In this case, the approximate product approach can easily be generalized to define regularized delta functions for $\Gamma$. Essentially, one needs to construct tangent line segments of $\Gamma$ which can easily be derived from $\phi_1$, $\phi_2$, and their gradients $\nabla\phi_1$ and $\nabla\phi_2$. Once the tangent line segments are defined, the integration procedure used in Section 3.1 can be applied. Further aspects about this topic will be reported in a future paper by the authors.

## 6. Conclusions

In [13], Tornberg and Engquist pointed out that the most common technique for regularization of Dirac delta functions in level set simulations is not consistent. This is shown both by analytical and numerical examples which results in O(1) errors.

In this paper, two new consistent techniques that can conveniently be used in connection to level set methods are introduced. Both techniques are based solely on the distance to the singularity and thus are independent of the grid. The first method uses a tensor product of regularized one-dimensional delta functions to construct approximation of the regularized delta function supported on a curve. This technique gives second-order convergence for singularities on smooth curves in numerical tests. We have proved it to be first-order accurate. The second technique uses a variable support of the regularization domain. The size of the support depends on the gradient of the level set function. This latter method is simpler but numerical examples suggest first-order convergence in most cases, which agrees with our theoretical results. We also demonstrate that the variable support size approach can be applied to regularize characteristic functions of sets, in which case yielding a second-order accurate approximation with minimal support of the regularization.

Both techniques can be applied to approximations of a class of PDEs with singular source terms. We have furthermore discussed a scaling that can be used if the level set function is not a signed distance function.

## Appendix A

We derive the the parameters $s_1, s_2, s_0^x$ and $s_0^y$ used in Section 3.1. Let $\nabla d(\Gamma, \mathbf{x})=(\cos(\theta), \sin(\theta))$. We consider $0 < \theta < \pi/2$. The cases when $\theta = 0$ or $\pi/2$ is trivial. Let $(x_*,\ y_*)$ denote $(d\cos\theta, d\sin\theta)$, and $\vec{\tau} = (\tau_1, \tau_2)$ denote $(-\sin\theta, \cos\theta)$. So $(x_*, y_*)$ is the closest point to $\mathbf{x}$ on $\Gamma$, and $\vec{\tau}$ is a tangent vector of $\Gamma$ at $x_*$, $y_*$. Furthermore, let $s_1^x$ and $s_1^y$ satisfy

$$\begin{cases} x_* + s_1^x\tau_1 = 1, \\ y_* + s_1^y\tau_2 = -1, \end{cases}$$

where $s_1^x$ and $s_1^y$ denotes the values when the line hits either the right or the bottom coordinate of the support. Therefore, we take the larger of the two values as $s_1$. It corresponds to the parameter at which $\Gamma$ first exits the support of $\tilde{\delta}_1^L$:

$$s_1 = \max(s_1^x, s_1^y) \quad \text{and} \quad \begin{cases} s_1^x = -\frac{1-d\cos\theta}{\sin\theta}, \\ s_1^y = -\frac{1+d\sin\theta}{\cos\theta}. \end{cases}$$

Similarly,

$$s_2 = \min(s_2^x, s_2^y) \quad \text{and} \quad \begin{cases} x_* + s_2^x\tau_1 = -1, \\ y_* + s_2^y\tau_2 = 1. \end{cases}$$

Next, we find the "time" when the line crosses the two axis. It is important as it determines the evaluation of $|X|$ or $|Y|$ in $\delta_\varepsilon^L$. Denote by $(x_0, 0)$ and $(0, y_0)$, respectively, the points of intersections with the $x$- and the $y$-axes, see Fig. 3. Then by definitions of $s_0^x$ and $s_0^y$:

$$\begin{cases} x_* + s_1^y\tau_1 = 0, \\ y_* + s_1^x\tau_2 = 0, \end{cases} \Rightarrow \begin{cases} s_0^x = d\cot\theta, \\ s_0^y = -d\tan\theta. \end{cases}$$

Under this construction, integration is only needed in the interval $K = [s_1, s_2]$. $s_0^y$ and $s_0^x$ denotes the sign change in $Y(s)$ and $X(s)$, respectively, and if they fall into $K$, we need to consider the the integration separately. This can be summarized into the following four cases: $s_0^x, s_0^y \notin K$, $s_0^y \notin K(s_1 < s_0^x < s_2)$, $s_0^x \notin Ks_1 < s_0^y < s_2$, and $s_1 < s_0^y < s_0^x < s_2$.

## References


[1] R.P. Beyer, R.J. LeVeque, Analysis of a one-dimensional model for the immersed boundary method, SIAM J. Numer. Anal. 29 (1992) 332–364.
[2] B. Burger, S. Osher, A survey on level set methods for inverse problems and optimal design, UCLA CAM Report No 04-02, 2004.
[3] L.-T. Cheng, Construction of shapes arising from the Minkowski problem using a level set approach, J. Sci. Comput. 19 (2003) 123–138.
[4] Li-Tien Cheng, The level set method applied to geometrically based motion, materials science, and image processing, PhD thesis, UCLA, 2000.
[5] J.B. Fraleigh, A First Course in Abstract Algebra, Addison-Wesley Publishing Co., 1989.
[6] Randall J. LeVeque, Zhi Lin Li, The immersed interface method for elliptic equations with discontinuous coefficients and singular sources, SIAM J. Numer. Anal. 31 (1994) 1019–1044.
[7] X.-D. Liu, R. Fedkiw, M. Kang, A boundary condition capturing method for Poisson's equation on irregular domains, J. Comput. Phys. 160 (1) (2000) 151–178.
[8] S.J. Osher, R.P. Fedkiw, Level Set Methods and Dynamic Implicit Surfaces, Springer, 2002.
[9] C.S. Peskin, The immersed boundary method, Acta Numer. 11 (2002) 479–517.
[10] J.A. Sethian, Level Set Methods and Fast Marching Methods. Evolving Interfaces in Computational Geometry, Fluid Mechanics, Computer Vision and Materials Science, Cambridge University Press, 1999.
[11] M. Sussman, P. Smereka, S. Osher, A level set method for computing solutions to incompressible two-phase flow, J. Comput. Phys. 114 (1994) 146–159.
[12] A.K. Tornberg, Multi-dimensional quadrature of singular and discontinuous functions, BIT 42 (2002) 644–669.
[13] A.-K. Tornberg, B. Engquist, Numerical approximations of singular source terms in differential equations, J. Comput. Phys. 200 (2004) 462–488.
[14] A.K. Tornberg, B. Engquist, Regularization techniques for numerical approximation of PDEs with singularities, J. Sci. Comput. 19 (2003) 527–552.
[15] A.K. Tornberg, B. Engquist, The segment projection method for interface tracking, Commun. Pure Appl. Math. 56 (2003) 47–79.
[16] G. Tryggvason, B. Bunner, A. Esmaeeli, D. Juric, N. Al-Rawahi, W. Tauber, J. Han, S. Nas, Y.J. Jan, A front-tracking method for the computations of multiphase flow, J. Comput. Phys. 169 (2001) 708–759.
[17] J. Waldén, On the approximation of singular source terms in differential equations, Numer. Meth. Part. D E 15 (1999) 503–520.
[18] H.-K. Zhao, T. Chan, B. Merriman, S. Osher, A variational level set approach to multiphase motion, J. Comput. Phys. 127 (1996) 179–195.